Mathematical Biosciences and Engineering

http://www.aimspress.com/journal/MBE

MBE, 16(6): 7327–7361.
DOI: 10.3934/mbe.2019366
Received: 12 April 2019
Accepted: 04 August 2019
Published: 09 August 2019

Research article

Global dynamics of non-smooth Filippov pest-natural enemy system with constant releasing rate

Hao Zhou, Xia Wang*and Sanyi Tang*

School of Mathematics and Information Science, Shaanxi Normal University, Xi'an, P.R. China.

* **Correspondence:** Email: sytang@snnu.edu.cn, xiawang@snnu.edu.cn; Tel: +862985310232.

Abstract: Modelling integrated pest management (IPM) with a threshold control strategy can be achieved with a non-smooth Filippov dynamical system coupled by an untreated subsystem and a treated subsystem which includes chemical and biological tactics. The releasing constant of natural enemies related to biological control generates the complex dynamics. Comprehensive qualitative analyses reveal that the treated subsystem exists with transcritical, saddle-node, Hopf and Bogdanov-Takens bifurcations, for which the threshold conditions and bifurcation curves are provided. Further, by applying techniques of non-smooth dynamical systems including the Filippov convex method and sliding bifurcation techniques, we first obtain the sliding dynamic equation, and then we analyze the existence and stability of regular/virtual equilibria, pseudo-equilibria, boundary equilibria, sliding segments and sliding bifurcations. In particular, if we choose the economic threshold (ET) as the bifurcation parameter, then interesting dynamical behaviors, including boundary equilibrium $\rightarrow$ pseudo-homoclinic $\rightarrow$ touching $\rightarrow$ buckling $\rightarrow$ crossing bifurcations, occur in succession. It is interesting to note that although the number of pests in the untreated subsystem could increase and exceed the economic injury level (EIL), the final size could be less than ET and stabilizes at a relative low level due to side effects of the pesticide on natural enemies. However, the side effects can be effectively avoided by increasing the releasing constant, which can maintain the number of pests below the EIL always and thus achieve the control purpose.

Keywords: Filippov system; integrated pest management; bifurcation; sliding dynamics; releasing constant

1. Introduction

Various modelling and analytical techniques have been widely employed to address the effectiveness of integrated pest management (IPM), which is a threshold control strategy [1–3] and it can be defined as follows: if the number of pests is below the economic threshold (ET), then the

integrated control strategy is not applied at all; above the ET then the integrated control measures including biological control and chemical control are applied with the aim of maintaining the number of pests below the economic injury level (EIL). In order to reveal the effectiveness of IPM, various mathematical models have been developed and studied based on the action mechanism of pesticides and the implementation of control strategies [4–10]. In particular, Filippov systems which are widely employed to depict intermittent control strategies and to describe many practical problems [7, 11–18], have been received much attention and investigated [7, 16–18]. However, most of the previous models strategy were designed to simplify the dynamic behavior of two subsystems without considering the constant releasing rate commonly used in IPM [17, 18]. In practical biological control methods, a constant releasing strategy is often used to facilitate operation and avoid monitoring the number of natural enemies, which has been proved to play an important role in the pest control [19–22].

In the present paper, a planar Filippov system formulated by two subsystems is proposed to reveal the effect of the constant releasing rate of natural enemy on the pest control, in which the discontinuity boundary or switching line is determined by the ET [23–27]. Therefore, the IPM strategy including spraying pesticide which the killing rate assumes to be proportional to the number of pests and releasing a constant number of natural enemies is applied once the number of the pest population exceeds the ET, otherwise the pest-natural enemy system is free from any control effects.

Based on the above facts, the pest-natural enemy interaction system without control measurements can be modelled by the classical Holling-II predator-prey model [28, 29] as follows:

$$\begin{cases} \dfrac{dx(t)}{dt} = rx - \dfrac{r}{K}x^2 - \dfrac{\beta xy}{1+\omega x}, \\ \dfrac{dy(t)}{dt} = \dfrac{\eta\beta xy}{1+\omega x} - \delta y, \end{cases} \tag{1.1}$$

where $x(t)$ and $y(t)$ represent the number of prey (pest) and predator (natural enemy), r is the intrinsic growth rate of the pest population and K represents its carrying capacity, $\dfrac{\beta x}{1+\omega x}$ denotes the Holling-II functional response function, which is a saturating function of the numbers of pests present, δ denotes the death rate of the natural enemy population, and η ($\eta \in (0, 1]$) denotes the conversion rate of the pest. The dynamics of this subsystem (also called an untreated subsystem) is well known and has been well studied [28], and will be summarized in the coming section.

The other subsystem (also called a treated subsystem) must be employed to model the artificial control strategies (spraying pesticides and releasing natural enemies), which can be represented as follows:

$$\begin{cases} \dfrac{dx(t)}{dt} = rx - \dfrac{r}{K}x^2 - \dfrac{\beta xy}{1+\omega x} - \alpha x, \\ \dfrac{dy(t)}{dt} = \dfrac{\eta\beta xy}{1+\omega x} - \delta_1 y + \tau, \end{cases} \tag{1.2}$$

where τ represents the releasing constant of natural enemies, α denotes the pest killing rate due to the spraying of pesticides, and $\delta_1 \geq \delta$ implies that the pesticide has side effects on the natural enemy. From a mathematical point of view, the essential difference between model (1.1) and model (1.2) is the constant release rate τ, which will result in rich dynamical behaviors and will be investigated in more detail in Section 3.

Combining the above two subsystems, we get the following non-smooth Filippov pest-natural enemy system with constant releasing rate as follows:

$$\begin{cases} \dfrac{dx(t)}{dt} = rx - \dfrac{r}{K}x^2 - \dfrac{\beta xy}{1+\omega x} - \epsilon\alpha x, \\ \dfrac{dy(t)}{dt} = \dfrac{\eta\beta xy}{1+\omega x} - (\delta + \epsilon h)y + \epsilon\tau \end{cases} \tag{1.3}$$

with

$$\begin{cases} \epsilon = 0, & x(t) < ET, \\ \epsilon = 1, & x(t) > ET, \end{cases}$$

where for convenience we denote $\delta_1 = \delta + h$ with $h \geq 0$. Note that if $\tau = 0$, then two subsystems (i.e., models (1.1) and (1.2) of Filippov system (1.3) have exactly the same dynamics, which have been widely used and investigated [24].

The objective of this paper is to systematically study the dynamical properties of non-smooth Filippov pest-natural enemy system with constant releasing rate and discuss bifurcations of model (1.3) depending on important parameters. This paper is organized as follows. In Section 2, we introduce the main definitions and terminologies of the generic second-order Filippov system. In Section 3, we systematically study the dynamical behavior of system (1.2) (i.e., subsystem S_2) and address how the constant releasing strategy affects the qualitative behaviors, which is crucial for analyzing Filippov system (1.3). The results show that system (1.2) exists rich dynamical behaviors including transcritical, saddle-node, Hopf and Bogdanov-Takens bifurcations [30, 31]. In Section 4, we study the existence and stability of the regular/virtual equilibria, pseudo-equilibria, sliding segments and sliding bifurcations of system (1.3) by employing the methods for non-smooth dynamical systems including the Filippov convex method and sliding bifurcation techniques [23, 26, 27, 32]. Particular attention is paid to the effect of the threshold level ET and releasing constant τ on the dynamical behavior of Filippov system (1.3) and successful pest control. The paper ends with brief conclusions and discussions.

2. Preliminaries

The generic second-order (i.e.,$X(t) \in R^2_+$) Filippov system can be defined as follows [12, 17, 23]:

$$\dot{X}(t) = \begin{cases} F_{S_1}(X), & X \in S_1, \\ F_{S_2}(X), & X \in S_2, \end{cases} \tag{2.1}$$

where $X(t) = \{x(t), y(t)\}^T$ and $R^2_+ = \{(x, y)|x \geq 0, y \geq 0\}$, and the regions S_1 and S_2 are separated by the discontinuity boundary Σ described by $H(X) = 0$, where $H(X)$ is a smooth scalar function with non-vanishing gradient $H_X(X)$ on Σ. For convenience, we call Filippov system (2.1) defined in region S_1 as subsystem S_1 and defined in region S_2 as subsystem S_2. Denote

$$\sigma(X) = \langle H_X(X), F_{S_1}(X)\rangle \cdot \langle H_X(X), F_{S_2}(X)\rangle,$$

where $\langle , \rangle$ is a Cartesian product in R^2 and $H_X(X)$ pointing to the region S_2 is called the positive direction. Based on the above concepts, we provide the necessary definitions of Filippov system (2.1) as follows:

Definition 1. If all these points $(x, y) \in \Sigma$ satisfy the condition $\sigma(X) \leq 0$, then we say that (x, y) belongs to the sliding segment, denoted by Σ_s. While the complement to Σ_s in Σ is called a crossing set, denoted by Σ_c. For the stability of the sliding segment, if

$$\langle H_X(X), F_{S_1}(X)\rangle > 0, \ \langle H_X(X), F_{S_2}(X)\rangle < 0,$$

then the sliding segment is stable. If

$$\langle H_X(X), F_{S_1}(X)\rangle < 0, \ \langle H_X(X), F_{S_2}(X)\rangle > 0,$$

then it is unstable.

Definition 2. If the point $R(x^*, y^*)$ of Filippov system (2.1) satisfies the following conditions

$$F_{S_1}(x^*, y^*) = 0 \text{ for } (x^*, y^*) \in S_1 \quad \text{or} \quad F_{S_2}(x^*, y^*) = 0 \text{ for } (x^*, y^*) \in S_2,$$

then it is called a regular equilibrium of Filippov system (2.1). Similarly, if it satisfies

$$F_{S_1}(x^*, y^*) = 0 \text{ for } (x^*, y^*) \in S_2 \quad \text{or} \quad F_{S_2}(x^*, y^*) = 0 \text{ for } (x^*, y^*) \in S_1,$$

then it is called a virtual equilibrium of Filippov system (2.1).

Definition 3. If the point $T(x^*, y^*)$ of Filippov system (2.1) satisfies

$$\langle H_X(x^*, y^*), F_{S_1}(x^*, y^*)\rangle = 0 \text{ for } (x^*, y^*) \in \Sigma_s \quad \text{or} \quad \langle H_X(x^*, y^*), F_{S_2}(x^*, y^*)\rangle = 0 \text{ for } (x^*, y^*) \in \Sigma_s,$$

then it is called a tangent point of Filippov system (2.1).

Definition 4. If the point $P(x^*, y^*)$ of Filippov system (2.1) satisfies

$$F_{S_1}(x^*, y^*) = 0 \text{ for } H(x^*, y^*) = 0 \quad \text{or} \quad F_{S_2}(x^*, y^*) = 0 \text{ for } H(x^*, y^*) = 0,$$

then it is called a boundary equilibrium of Filippov system (2.1).

Note that the three points $P(x^*, y^*)$, $T(x^*, y^*)$ and $R(x^*, y^*)$ may collide together for some critical cases, and for more definitions and properties of Filippov system (2.1) please see [12, 17, 23]. Now let us turn to non-smooth Filippov system (1.3), which can be represented as:

$$\dot{X}(t) = \begin{cases} f_1(x, y), & (x, y) \in S_1, \\ f_2(x, y), & (x, y) \in S_2, \end{cases} \tag{2.2}$$

where the discontinuity boundary is $\Sigma = \{(x, y) \in R^2_+ | H(x, y) = 0\}$ and $H(x, y) = x - ET$, which separates the two regions $S_1 = \{(x, y) \in R^2_+ | H(x, y) < 0\}$ and $S_2 = \{(x, y) \in R^2_+ | H(x, y) > 0\}$. The vector field for subsystem S_1 is

$$f_1(x, y) = \left\{ rx - \frac{r}{K}x^2 - \frac{\beta xy}{1 + \omega x}, \quad \frac{\eta\beta xy}{1 + \omega x} - \delta y \right\}^T$$

and the vector field for subsystem S_2 is

$$f_2(x, y) = \left\{ rx - \frac{r}{K}x^2 - \frac{\beta xy}{1 + \omega x} - \alpha x, \quad \frac{\eta\beta xy}{1 + \omega x} - \delta_1 y + \tau \right\}^T.$$

The dynamics of two subsystems S_1 and S_2 are crucial for analyzing the global dynamics of Filippov system (2.2), and the complete dynamical behavior of subsystem S_1 has been discussed in more detail in the literature [28]. That is to say, subsystem S_1 always exists with a trivial equilibrium $R^0_{S_1}(0,0)$ which is unstable, and a boundary equilibrium $R^1_{S_1}(K,0)$ which is globally stable if $\frac{\delta}{\eta\beta-\delta\omega} \geq K$ or $\frac{\delta}{\eta\beta-\delta\omega} <$ 0holds true. Meanwhile, subsystem S_1 exists with a positive equilibrium $R^2_{S_1}\left(\frac{\delta}{\eta\beta-\delta\omega}, \frac{r\eta(K\eta\beta-K\delta\omega-\delta)}{K(\eta\beta-\delta\omega)^2}\right)$ if and only if $0 < \frac{\delta}{\eta\beta-\delta\omega} < K$, which is a globally stable node or focus provided that $\omega K \leq \frac{\eta\beta+\delta\omega}{\eta\beta-\delta\omega}$. Otherwise, it is an unstable node or focus and there exists a unique and stable limit cycle.

However, the dynamical behavior of subsystem S_2 has not been addressed so far because the constant releasing rate will bring some challenges for qualitative analysis. Although a similar model was investigated in reference [31], we realize that the sign of the constant τ (minus τ was used in [31]) could result in different dynamics including the existence and stability of equilibria and various bifurcations. Thus, we first carry out qualitative analyses for subsystem S_2 in the following.

3. The dynamics of subsystem S_2

In this section, we will investigate the dynamical behavior of subsystem S_2 and focus on the effect of parameter τ on the dynamics, i.e., the effect of the control strategy (releasing natural enemies) in the pest control. For convenience, we rewrite the subsystem S_2 as follows:

$$\begin{cases} \dfrac{dx(t)}{dt} = rx - \dfrac{r}{K}x^2 - \dfrac{\beta xy}{1+\omega x} - \alpha x \doteq P_1(x,y), \\ \dfrac{dy(t)}{dt} = \dfrac{\eta\beta xy}{1+\omega x} - \delta_1 y + \tau \doteq Q_1(x,y), \end{cases} \tag{3.1}$$

here we assume that $r > \alpha$.

3.1. Existence and stability of the equilibria of system (3.1)

Firstly, let us begin to determine the location and number of the equilibria of system (3.1) in R^2_+. It is easy to check that the point $R^0_{S_2}(0, \frac{\tau}{\delta_1})$ is always the boundary equilibrium of system (3.1). In the following, we mainly focus on the existence of the positive equilibria of system (3.1).

It is clear that equations

$$\begin{cases} P_1(x,y) = 0, \\ Q_1(x,y) = 0, \end{cases} \tag{3.2}$$

have at most two positive real solutions:

$$x_1 \doteq \frac{KR_2 - K\sqrt{\Delta}}{2rR_0},\ y_1 \doteq (r_1 - \frac{r}{K}x_1)\frac{1+\omega x_1}{\beta}$$

and

$$x_2 \doteq \frac{KR_2 + K\sqrt{\Delta}}{2rR_0},\ y_2 \doteq (r_1 - \frac{r}{K}x_2)\frac{1+\omega x_2}{\beta},$$

where

$$r_1 \doteq r-\alpha,\ \ R_0 \doteq \eta\beta - \delta_1\omega,\ \ R_1 \doteq \beta\tau - r_1\delta_1,\ \ R_2 \doteq r_1(\eta\beta - \delta_1\omega) + \frac{r\delta_1}{K} \ \text{ and } \ \Delta \doteq R_2^2 + \frac{4rR_0R_1}{K}.$$

That is to say, system (3.1) has at most two positive equilibria in R^2_+, denoted by $R^1_{S_2}(x_1, y_1)$ and $R^2_{S_2}(x_2, y_2)$. And we have the following simple theorem which describes the number and location of equilibria of system (3.1). The proof is omitted.

Lemma 3.1. For system (3.1), with R_0, R_1, R_2 and Δ defined as above, we have:

(i) when $R_0 > 0$, system (3.1) has at most two equilibria in R^2_+ and it has the following possibilities:

- **(a)** if $R_1 > 0$ holds, then system (3.1) has a unique equilibrium $R^0_{S_2}$;
- **(b)** if $R_1 < 0$ holds, then system (3.1) has two equilibria $R^0_{S_2}$ and $R^1_{S_2}$;
- **(c)** if $R_1 = 0$ holds, then $R^0_{S_2}$ and $R^1_{S_2}$ coalesce at a boundary equilibrium of multiplicity 2.

(ii) when $R_0 < 0$, system (3.1) has at most three equilibria in R^2_+ and it has the following possibilities:

- **(a)** if $R_1 > 0$, $R_2 < 0$ and $\Delta > 0$ hold, then system (3.1) has three equilibria $R^0_{S_2}$, $R^1_{S_2}$ and $R^2_{S_2}$;
- **(b)** if $R_1 > 0$, $R_2 < 0$ and $\Delta = 0$ hold, then $R^1_{S_2}$ and $R^2_{S_2}$ coalesce at a positive equilibrium of multiplicity 2, which coexists with $R^0_{S_2}$;
- **(c)** if $R_1 > 0$, $R_2 < 0$ and $\Delta < 0$ hold, then system (3.1) has a unique equilibrium $R^0_{S_2}$;
- **(d)** if $R_1 < 0$ holds, then system (3.1) has two equilibria $R^0_{S_2}$ and $R^1_{S_2}$;
- **(e)** if $R_1 = 0$ and $R_2 < 0$ hold, then $R^0_{S_2}$ and $R^2_{S_2}$ coalesce at a boundary equilibrium of multiplicity 2, which coexists with $R^1_{S_2}$;
- **(f)** if $R_1 = 0$ and $R_2 > 0$ hold, then $R^0_{S_2}$ and $R^1_{S_2}$ coalesce at a boundary equilibrium of multiplicity 2, and $R^2_{S_2}$ disappears in this case;
- **(g)** if $R_1 = 0$ and $R_2 = 0$ hold, then $R^0_{S_2}$, $R^1_{S_2}$ and $R^2_{S_2}$ coalesce at a boundary equilibrium of multiplicity 3.

Next we discuss the possible phase portraits of system (3.1) and analyze the stability of equilibria according to Lemma 3.1.

3.1.1. Case (i): $R_0 > 0$

In this case, system (3.1) has at most two equilibria $R^1_{S_2}(x_1, y_1)$ and $R^0_{S_2}(0, \frac{\tau}{\delta_1})$ in R^2_+, and we can get the following results.

Theorem 3.1. If $R_0 > 0$ and $R_1 > 0$, then system (3.1) exists with a boundary equilibrium $R^0_{S_2}$ in R^2_+, which is a globally asymptotically stable node.

Proof. In this case, system (3.1) only has a boundary equilibrium $R^0_{S_2}(0, \frac{\tau}{\delta_1})$ in R^2_+. And the Jacobian matrix at $R^0_{S_2}$ is given by

$$\mathbf{A}_{R^0_{S_2}} = \begin{pmatrix} r_1 - \frac{2rx}{K} - \frac{\beta y}{(1+\omega x)^2} & -\frac{\beta x}{1+\omega x} \\ \frac{\eta\beta y}{(1+\omega x)^2} & \frac{\eta\beta x}{1+\omega x} - \delta_1 \end{pmatrix}\Bigg|_{R^0_{S_2}} = \begin{pmatrix} r_1 - \frac{\beta\tau}{\delta_1} & 0 \\ \frac{\eta\beta\tau}{\delta_1} & -\delta_1 \end{pmatrix}.$$

The corresponding characteristic equation is

$$|\mathbf{A}_{R^0_{S_2}} - \lambda\mathbf{E}| = \lambda^2 + p_{R^0_{S_2}}\lambda + q_{R^0_{S_2}} = 0,$$

where $q_{R^0_{S_2}} \doteq \beta\tau - r_1\delta_1 = R_1 > 0$, $p_{R^0_{S_2}} \doteq \delta_1 + \frac{\beta\tau}{\delta_1} - r_1 > 0$ and $p^2_{R^0_{S_2}} - 4q_{R^0_{S_2}} = (\delta_1 - \frac{\beta\tau}{\delta_1} + r_1)^2 > 0$. This means that $R^0_{S_2}$ is a locally asymptotically stable node. Especially, when $\tau = 0$, we have $q_{R^0_{S_2}} = -r_1\delta_1 < 0$ which indicates that $R^0_{S_2}$ is an unstable saddle.

Now we begin to discuss the global stability of $R^0_{S_2}$. In the first quadrant, the two non-zero isoclines $L^1_{S_2}$ and $L^2_{S_2}$ of system (3.1) divide R^2_+ into four regions:

$$I = \{(x,y)|P_1(x,y) < 0,\ Q_1(x,y) < 0\};\ II = \{(x,y)|P_1(x,y) > 0,\ Q_1(x,y) > 0\};$$

$$III = \left\{(x,y)|P_1(x,y) < 0,\ Q_1(x,y) > 0,\ x \le \frac{\delta_1}{R_0}\right\};$$

$$IV = \left\{(x,y)|P_1(x,y) < 0,\ Q_1(x,y) > 0,\ x > \frac{\delta_1}{R_0}\right\},$$

at which the signs of two functions $P_1(x,y)$ and $Q_1(x,y)$ are clear.

It is known that system (3.1) does not exist with any other equilibria in R^2_+ except $R^0_{S_2}$. From Figure 1, we can see that the trajectory $\{x(t,x_0,y_0), y(t,x_0,y_0)\}$ of system (3.1) will approach the boundary equilibrium $R^0_{S_2}$ directly, or intersects with the non-zero isoclines $L^1_{S_2}$ or $L^2_{S_2}$ firstly, and then tends to the boundary equilibrium $R^0_{S_2}$ as $t \to +\infty$ for any initial value $(x_0,y_0) \in I \bigcup II \bigcup III$.

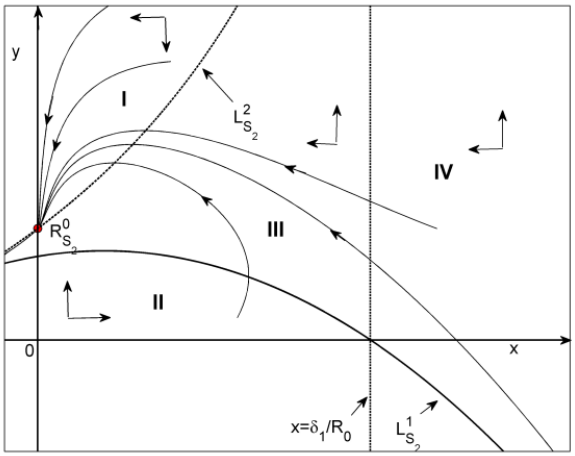

Figure 1. Illustration of the global stability of the boundary equilibrium $R^0_{S_2}$, where the vector field of system (3.1) and its trajectories are shown.

By a simple calculation, we have

$$\left|\frac{dy}{dx}\right| = \left|\frac{Q_1(x,y)}{P_1(x,y)}\right| = \left|\frac{\eta\beta - \delta_1\omega}{\beta}\right| \cdot \left|\frac{1 - \frac{\frac{\delta_1}{\eta\beta-\delta_1\omega}}{x} + \frac{\frac{\delta_1}{\eta\beta-\delta_1\omega}(\frac{\tau}{\beta}+\frac{\tau\omega}{\beta}x)}{xy}}{1 + \frac{\frac{r\omega}{\beta K}x^2 - \frac{r_1\omega - \frac{r}{K}}{\beta} - \frac{r_1}{\beta}}{xy}}\right| < \frac{R_0}{\beta}$$

for all $(x,y) \in IV$ and $y \gg 1$. That is to say, the trajectories of system (3.1) can not always remain to the right of the line $x = \frac{\delta_1}{R_0}$, which indicates that the trajectories starting from the region IV must

cross the line $x = \frac{\delta_1}{R_0}$ and enter into the region III, and then approach the boundary equilibrium $R^0_{S_2}$ as $t \to +\infty$. Thus, the boundary equilibrium $R^0_{S_2}$ is a globally stable node. This completes the proof.

Theorem 3.2. If $R_0 > 0$ and $R_1 = 0$, then system (3.1) does not exist with a positive equilibrium, and the boundary equilibrium $R^0_{S_2}$ is a saddle-node of codimension 1.

Proof. Note that if $R_1 = 0$, then the boundary equilibrium $R^0_{S_2}$ collides with the positive equilibrium $R^1_{S_2}$ in R^2_+, which is a high order singular point. Translating the boundary equilibrium $R^0_{S_2}(0, \frac{\tau}{\delta_1})$ to the origin by making the change of variables $u = x$ and $v = y - \frac{\tau}{\delta_1}$, renaming (u, v) as (x, y) and expanding the right-hand side of system (3.1) in a Taylor series about the origin, then we can obtain

$$\begin{cases} \dfrac{dx}{dt} = (r_1\omega - \dfrac{r}{K})x^2 - \beta xy - r_1\omega^2 x^3 + \beta\omega x^2 y + M_1(x, y), \\ \dfrac{dy}{dt} = r_1\eta x - \delta_1 y - r_1\eta\omega x^2 + \eta\beta xy + r_1\eta\omega^2 x^3 - \eta\beta\omega x^2 y + M_2(x, y), \end{cases} \tag{3.3}$$

where $M_1(x, y)$ and $M_2(x, y)$ are C^∞ functions in (x, y) at least of the fourth order.

Notice that $\delta_1 > 0$, making the following change of variables

$$u = x,\ v = r_1\eta x - \delta_1 y$$

and renaming (u, v) as (x, y), then system (3.3) becomes

$$\begin{cases} \dfrac{dx}{dt} = -\dfrac{R_2}{\delta_1}x^2 + \dfrac{\beta}{\delta_1}xy + \dfrac{r_1\omega R_0}{\delta_1}x^3 - \dfrac{\beta\omega}{\delta_1}x^2 y + M_3(x, y) \doteq P_2(x, y), \\ \dfrac{dy}{dt} = -\delta_1 y - \dfrac{r_1\eta}{\delta_1}(R_2 + \delta_1 R_0)x^2 + (1 + \dfrac{r_1}{\delta_1})\eta\beta xy + r_1\eta\omega R_0(1 + \dfrac{r_1}{\delta_1})x^3 - \eta\beta\omega(1 + \dfrac{r_1}{\delta_1})x^2 y + M_4(x, y) \\ \quad \doteq Q_2(x, y) - \delta_1 y, \end{cases} \tag{3.4}$$

where $R_2 > 0$, and $M_3(x, y)$, $M_4(x, y)$ are C^∞ functions in (x, y) at least of the fourth order. Solving the equation $-\delta_1 y + Q_2(x, y) = 0$, we can obtain the implicit solution

$$\phi(x) \doteq -\frac{r_1\eta}{\delta_1^2}(R_2 + \delta_1 R_0)x^2 + O(x^3). \tag{3.5}$$

where $R_2 + \delta_1 R_0 > 0$. And substituting $\phi(x)$ into $P_2(x, y)$, which can be written in the form

$$\psi(x) \doteq P_2(x, \phi(x)) = -\frac{R_2}{\delta_1}x^2 + O(x^3). \tag{3.6}$$

According to Theorems 7.1–7.3 in [30], it is easy to obtain that $R^0_{S_2}$ is a saddle-node of codimension 1 if $R_0 > 0$ and $R_1 = 0$. The proof is completed.

In the following, we discuss the stability of the positive equilibria of system (3.1). For convenience, we first denote

$$R_3 \doteq \frac{K(\eta\beta - \delta_1\omega - \frac{r}{K} + r_1\omega)x_1}{K\delta_1 + 2r\omega x_1^2} \quad \text{and} \quad R_4 \doteq \frac{(\eta\beta - \delta_1\omega - \frac{r}{K} + r_1\omega)\sqrt{2r\delta_1\omega K}}{4r\delta_1\omega}.$$

Moreover, we have the following main results.

Theorem 3.3. If $R_0 > 0$ and $R_1 < 0$, then system (3.1) has an unstable boundary equilibrium $R^0_{S_2}$ and a positive equilibrium $R^1_{S_2}$ in R^2_+. Further, if $R_3 < 1$, then $R^1_{S_2}$ is a locally stable node (or a focus), and it is globally stable provided that $R_4 < 1$.

Proof. For the boundary equilibrium $R^0_{S_2}(0, \frac{\tau}{\delta_1})$, we have

$$|\mathbf{A}_{R^0_{S_2}} - \lambda \mathbf{E}| = \lambda^2 + p_{R^0_{S_2}} \lambda + q_{R^0_{S_2}} = 0$$

with $q_{R^0_{S_2}} = \beta\tau - r_1\delta_1 = R_1 < 0$, which indicates that $R^0_{S_2}$ is an unstable saddle.

For the positive equilibrium $R^1_{S_2}(x_1, y_1)$, the characteristic equation is as follows:

$$|\mathbf{A}_{R^1_{S_2}} - \lambda \mathbf{E}| = \lambda^2 + p_{R^1_{S_2}} \lambda + q_{R^1_{S_2}} = 0, \tag{3.7}$$

where

$$p_{R^1_{S_2}} = \frac{1}{1 + \omega x_1} \left[\frac{2r\omega}{K} x_1^2 - (\eta\beta - \delta_1\omega - \frac{r}{K} + r_1\omega)x_1 + \delta_1 \right] \tag{3.8}$$

and

$$q_{R^1_{S_2}} = \frac{2rR_0x_1}{K(1 + \omega x_1)} \left[\frac{KR_2}{2rR_0} - x_1 \right]. \tag{3.9}$$

Obviously, $q_{R^1_{S_2}} > 0$. It follows from (3.8) that if

$$\eta\beta - \delta_1\omega - \frac{r}{K} + r_1\omega < \frac{K\delta_1 + 2r\omega x_1^2}{Kx_1}$$

holds true, which is equivalent to the following inequality

$$\frac{K(\eta\beta - \delta_1\omega - \frac{r}{K} + r_1\omega)x_1}{K\delta_1 + 2r\omega x_1^2} < 1, \text{ i.e., } R_3 < 1,$$

then $p_{R^1_{S_2}} > 0$ and consequently $R^1_{S_2}$ is a locally asymptotically stable node (or focus).

In order to show the global stability of $R^1_{S_2}$, for simplifying the calculations, we consider a polynomial system, which has the same equilibria $R^0_{S_2}$, $R^1_{S_2}$, $R^2_{S_2}$ and dynamics as system (3.1) for $x > -\frac{1}{\omega}$. To do this, multiplying both sides of system (3.1) by the function $\frac{1+\omega x}{\beta}$ and introducing a new time variable τ by $dt = \frac{1+\omega x}{\beta} d\tau$ yield the following polynomial system:

$$\begin{cases} \dfrac{dx(t)}{d\tau} = x(a_1 + a_2x - a_3x^2 - y) \doteq P_2(x, y), \\ \dfrac{dy(t)}{d\tau} = b_1xy - b_2y + b_3 + b_4x \doteq Q_2(x, y), \end{cases} \tag{3.10}$$

where $a_1 = \frac{r_1}{\beta}, a_2 = \frac{r_1\omega - \frac{r}{K}}{\beta}, a_3 = \frac{r\omega}{\beta K}, b_1 = \frac{\eta\beta - \delta_1\omega}{\beta}, b_2 = \frac{\delta_1}{\beta}, b_3 = \frac{\tau}{\beta}, b_4 = \frac{\tau\omega}{\beta}$, and $a_1, a_3, b_1, b_2, b_3, b_4$ are all positive constants, the signs of a_2 could vary.

Let $B(x, y) = x^{-1}$ be the Dulac function [30], by a simple calculation, we can obtain that

$$\frac{\partial BP_2(x, y)}{\partial x} = \frac{\partial(a_1 + a_2x - a_3x^2 - y)}{\partial x} = a_2 - 2a_3x,$$

$$\frac{\partial BQ_2(x,y)}{\partial y} = \frac{\partial(b_1 y - b_2 x^{-1} y + b_3 x^{-1} + b_4)}{\partial y} = b_1 - b_2 x^{-1},$$

$$D \doteq \frac{\partial BP_2}{\partial x} + \frac{\partial BQ_2}{\partial y} = -x^{-1}[2a_3 x^2 - (a_2 + b_1)x + b_2] \doteq -x^{-1} g(x). \tag{3.11}$$

It follows from (3.11) that if

$$\Delta_2 \doteq (a_2 + b_1)^2 - 8a_3 b_2 = (\frac{\eta\beta - \delta_1\omega - \frac{r}{K} + r_1\omega}{\beta})^2 - \frac{8r\delta_1\omega}{\beta^2 K} < 0,$$

i.e.,

$$-2\sqrt{\frac{2r\delta_1\omega}{K}} < \eta\beta - \delta_1\omega - \frac{r}{K} + r_1\omega < 2\sqrt{\frac{2r\delta_1\omega}{K}},$$

then the function $g(x) = 2a_3x^2 - (a_2 + b_1)x + b_2 > 0$ for all $x \in R$. That is to say, $D < 0$ for all $(x, y) \in R^2_+$. Note that for the function $g(x)$, it is easy to see that when $a_2 + b_1 < 0$, i.e., $\eta\beta - \delta_1\omega - \frac{r}{K} + r_1\omega < 0$, we have $g(x) > 0$ for all $x \geq 0$ and consequently $D < 0$ for all $(x, y) \in R^2_+$.

Therefore, according to the above analyses, we can conclude that if

$$\eta\beta - \delta_1\omega - \frac{r}{K} + r_1\omega < 2\sqrt{\frac{2r\delta_1\omega}{K}},$$

which is equivalent to the inequality

$$\frac{(\eta\beta - \delta_1\omega - \frac{r}{K} + r_1\omega)\sqrt{2r\delta_1\omega K}}{4r\delta_1\omega} < 1, \text{ i.e., } R_4 < 1,$$

then $D < 0$, and consequently system (3.10) does not exist with any periodic solutions lying in the interior of R^2_+, which indicates that $R^1_{S_2}$ is globally stable, as shown in Figure 2A. This completes the proof.

Remark It is easy to see that the condition $R_4 < 1$ is stronger than the inequality $R_3 < 1$, which reveals that the local stability of the equilibrium $R^1_{S_2}$ does not indicate the global stability. However, extensive numerical investigations show that $R^1_{S_2}$ is a globally stale equilibrium provided that $R_3 < 1$, but unfortunately we have no way to prove it at present.

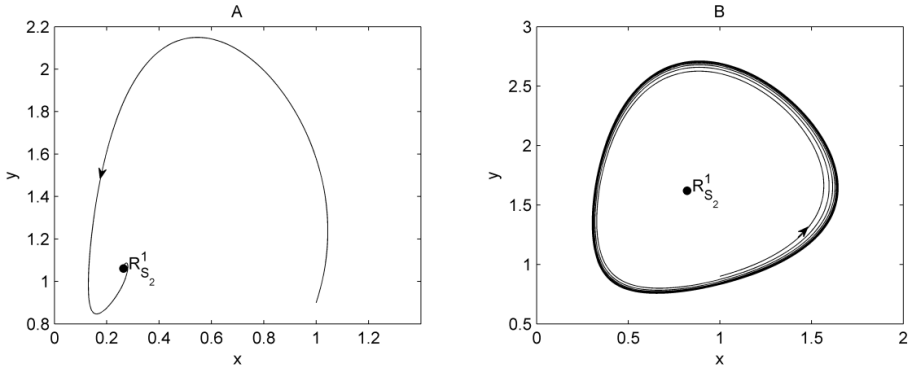

Figure 2. Illustrations of the global stability of the positive equilibrium $R^1_{S_2}$ and the existence of a limit cycle. The parameter values are fixed as follows: $K = 8$, $r = 3$, $\beta = 3$, $\delta_1 = 2$, $\omega = 2/3$, $\eta = 5/6$. A: $\alpha = 1.2$, $\tau = 0.8$ with $R_4 < 1$. B: $\alpha = 0.8$, $\tau = 0.2$ with $R_3 > 1$.

Theorem 3.4. If $R_3 > 1$ holds true, then system (3.10) has at least one limit cycle in the interior of R_+^2.

Proof. Based on the analyses in Theorem 3.3, we know that if $R_3 > 1$, then the positive equilibrium $R_{S_2}^1$ is an unstable focus (or node). To show the existence of a limit cycle, we define the following four lines:

$$L_1 : x - \frac{r_1 K}{r} = 0;\ L_2 : x = 0;\ L_3 : y = 0 \text{ and } L_4 : x + \frac{1}{b_1} y + P = 0,$$

which form a closed region G, where P is a constant and the positive equilibrium $R_{S_2}^1$ belongs to G. For all $x \in \left[0, \frac{r_1 K}{r}\right]$ and $y > 0$, we have

$$\frac{dL_1}{dt}\Big|_{x=\frac{r_1 K}{r}} = -\frac{r_1 K}{r} y < 0,$$

which indicates that if the trajectories of system (3.10) intersect with the line L_1, it will pass from the right side of the line L_1 to the left, entering into the region G. Moreover, it follows from

$$\frac{dL_3}{dt}\Big|_{y=0} = b_3 + b_4 x > 0$$

that if the trajectories of system (3.10) intersect with the line L_3, it will pass from the below of the line L_3 to the top, entering into the region G. Further, by a simple calculation, we have

$$\frac{dL_4}{dt}\Big|_{y=-b_1(x+P)} = x\left(a_1 + a_2 x - a_3 x^2 + \frac{b_4}{b_1}\right) + (1 + b_2) P + \frac{b_3}{b_1}.$$

Thus, if we choose the constant P such that $P < -\max\left\{\frac{1}{1+b_2}[x(a_1 + a_2 x - a_3 x^2 + \frac{b_4}{b_1}) + \frac{b_3}{b_1}]\right\}$, then $\frac{dL_4}{dt}\Big|_{y=-b_1(x+P)} < 0$. That is to say, if the trajectories of system (3.10) intersect with the line L_4, it will pass from the top of the line L_4 to below it, entering into the region G.

Note that L_2 is one of the trajectories of system (3.10), which approaches the boundary equilibrium $R_{S_2}^0$ and the trajectories initiating from region G will remain in it, i.e., L_1, L_2, L_3 and L_4 form a Bendixson curve. Thus, according to the Poincaré-Bendixson Theorem [30], system (3.10) has at least one limit cycle around the positive equilibrium $R_{S_2}^1$, as shown in Figure 2B. This completes the proof.

Unfortunately, we can not employ the main results shown in literature [30] to address the uniqueness of the limit cycle. Therefore, in the following, we further consider the uniqueness and stability of the limit cycle through bifurcation analyses in subsection 3.2.

3.1.2. Case (ii): $R_0 < 0$

In this case, system (3.1) has at most three equilibria in R_+^2 including two positive equilibria $R_{S_2}^1(x_1, y_1)$ and $R_{S_2}^2(x_2, y_2)$, and a boundary equilibrium $R_{S_2}^0(0, \frac{\tau}{\delta_1})$ which is a stable node if $R_1 > 0$ and it is an unstable saddle if $R_1 < 0$. Based on the characteristic equation (3.7), for $R_{S_2}^1$ and $R_{S_2}^2$, we have

$$p_{R_{S_2}^1} = \frac{1}{1 + \omega x_1}\left[\frac{2rw}{K} x_1^2 - (\eta\beta - \delta_1\omega - \frac{r}{K} + r_1\omega) x_1 + \delta_1\right], q_{R_{S_2}^1} = \frac{x_1\sqrt{\Delta}}{1 + \omega x_1}$$

and

$$p_{R^1_{S_2}} = \frac{1}{1+\omega x_2}\left[\frac{2rw}{K}x_2^2 - (\eta\beta - \delta_1\omega - \frac{r}{K} + r_1\omega)x_2 + \delta_1\right], q_{R^1_{S_2}} = -\frac{x_2\sqrt{\Delta}}{1+\omega x_2}.$$

Obviously, $q_{R^1_{S_2}} > 0$ and $q_{R^2_{S_2}} < 0$. That is to say, $R^2_{S_2}$ is an unstable saddle and $R^1_{S_2}$ is an elementary and not saddle-type equilibrium. Further, we have the following results:

Theorem 3.5. If $R_0 < 0$, $R_1 > 0$, $R_2 < 0$ and $\Delta > 0$, then system (3.1) exists with three equilibria: $R^0_{S_2}$, $R^1_{S_2}$ and $R^2_{S_2}$. Further, $R^0_{S_2}$ is a locally stable node, $R^2_{S_2}$ is an unstable saddle and $R^1_{S_2}$ is a node (or a focus) which is locally stable provided $R_3 < 1$.

Theorem 3.6. If $R_0 < 0$, $R_1 > 0$, $R_2 < 0$ and $\Delta = 0$, then system (3.1) exists with a locally stable boundary equilibrium $R^0_{S_2}$. Moreover, $R^1_{S_2}$ collides with $R^2_{S_2}$, which is a saddle-node of codimension 1 when $R_3 \neq 1$.

Theorem 3.7. If $R_0 < 0$, $R_1 > 0$, $R_2 < 0$ and $\Delta < 0$, then system (3.1) exists with a boundary equilibrium $R^0_{S_2}$, which is a globally asymptotically stable node.

Theorem 3.8. If $R_0 < 0$ and $R_1 < 0$, then system (3.1) has an unstable boundary equilibrium $R^0_{S_2}$ and a positive equilibrium $R^1_{S_2}$. Further, if $R_3 < 1$, then $R^1_{S_2}$ is a locally stable node (or a focus), and it is globally stable provided that $R_4 < 1$.

Theorem 3.9. If $R_0 < 0$ and $R_1 = 0$, then the boundary equilibrium $R^0_{S_2}$ is a high order singular point. More precisely,

(i) $R^0_{S_2}$ is a saddle-node of codimension 1 if $R_2 \neq 0$;

(ii) $R^0_{S_2}$ is an unstable saddle of codimension 2 if $R_2 = 0$.

Proof. The proof of the conclusion (i) is similar to that for Theorem 3.2, we discuss the conclusion (ii) in the following.

For system (3.4), when $R_2 = 0$, then it can be represented as

$$\begin{cases} \dfrac{dx}{dt} = \dfrac{\beta}{\delta_1}xy + \dfrac{r_1\omega R_0}{\delta_1}x^3 - \dfrac{\beta\omega}{\delta_1}x^2y + M_3(x,y) \doteq P_2(x,y), \\ \dfrac{dy}{dt} = -\delta_1 y - r_1\eta R_0 x^2 + (1+\dfrac{r_1}{\delta_1})\eta\beta xy + r_1\eta\omega R_0(1+\dfrac{r_1}{\delta_1})x^3 - \eta\beta\omega(1+\dfrac{r_1}{\delta_1})x^2y + M_4(x,y) \\ \quad \doteq Q_2(x,y) - \delta_1 y, \end{cases} \tag{3.12}$$

Solving the equation $-\delta_1 y + Q_2(x,y) = 0$, we obtain the implicit solution

$$\phi(x) \doteq -\frac{r_1\eta R_0}{\delta_1}x^2 + O(x^3). \tag{3.13}$$

Then substituting $\phi(x)$ into $P_2(x,y)$, which can be written in the form

$$\psi(x) \doteq P_2(x,\phi(x)) = -\frac{r_1R_0^2}{\delta_1^2}x^3 + O(x^4). \tag{3.14}$$

According to Theorems 7.1–7.3 in [30], it is easy to obtain that $R^0_{S_2}$ is an unstable saddle of codimension 2 if $R_0 < 0$, $R_1 = 0$ and $R_2 = 0$. The proof is completed.

3.2. The Bifurcations of system (3.1)

In this section, we will discuss various possible bifurcations of system (3.1) including transcritical, saddle-node, Hopf and Bogdanov-Takens bifurcations.

3.2.1. Transcritical bifurcation

It follows from Lemma 3.1 and Theorems 3.1–3.3, that the positive equilibrium $R^1_{S_2}$ collides with the boundary equilibrium $R^0_{S_2}$ when $R_1 = 0$, and solving $R_1 = 0$ with respect to τ, we have $\tau^*_0 = \frac{r_1\delta_1}{\beta}$. Moreover, if $\tau < \tau^*_0$, then system (3.1) has two equilibria: $R^1_{S_2}$ which is a stable node (or focus) provided that $R_3 < 1$, and $R^0_{S_2}$ which is an unstable saddle. If $\tau > \tau^*_0$, then $R^1_{S_2}$ becomes negative which is unstable, and $R^0_{S_2}$ becomes a stable node, which indicates that the transcritical bifurcation occur at τ^*_0, as shown in Figure 3. Further, we can obtain that

$$TB = \{(r, \alpha, \beta, \eta, \omega, \tau, \delta_1)|\ R_0 > 0, \tau = \tau^*_0\}$$

is a transcritical bifurcation surface. This indicates that there exists a critical releasing rate τ^*_0 such that the pests and natural enemies coexist in the form of a positive equilibrium or a periodic orbit with a finite period when the releasing rate $\tau < \tau^*_0$, and the pest population goes extinct when the releasing rate $\tau > \tau^*_0$.

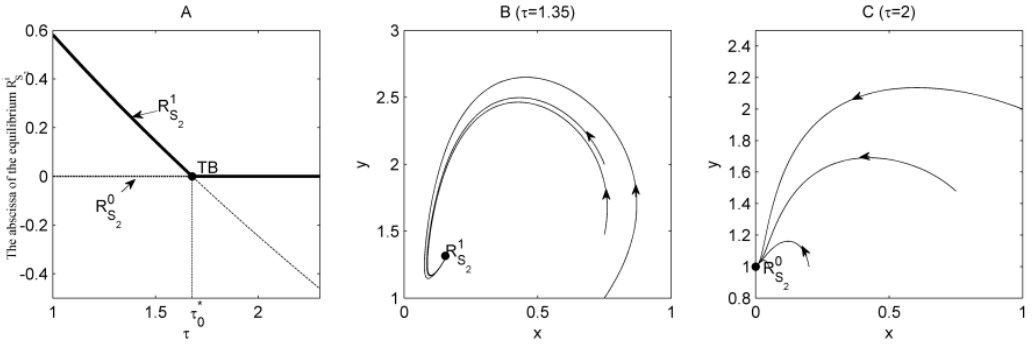

Figure 3. Bifurcation diagrams with respect to parameter τ, where TB denotes the transcritical bifurcation, and the solid black curve indicates that the equilibrium is stable, otherwise it is unstable. The parameter values are fixed as follows: $K = 7$, $r = 3$, $\beta = 2.8$, $\delta_1 = 2$, $\omega = 0.66$, $\eta = 0.88$, $\alpha = 0.65$. B: $\tau = 1.35$. C: $\tau = 2$.

3.2.2. Saddle-node bifurcation

From Lemma 3.1 and Theorems 3.5–3.7, we can obtain that

$$SN = \{(r, \alpha, \beta, \eta, \omega, \tau, \delta_1, K)|\ R_0 < 0, R_1 > 0, R_2 < 0 \text{ and } \Delta = 0\}$$

is a saddle-node bifurcation surface. When the parameters pass from the one side of the surface to the other, the number of positive equilibria of system (3.1) changes from zero to two, and the two positive equilibria are saddle and node, as shown in Figure 4. Especially, if we choose τ as bifurcation

parameter and solving $\Delta = 0$ with respect to τ, we have $\tau_1^* = \frac{K[\frac{r\delta_1}{K} - r_1 R_0]^2}{4\beta r R_0}$ and the above saddle-node bifurcation surface can be represented as

$$SN = \{(r, \alpha, \beta, \eta, \omega, \tau, \delta_1, K) | \, R_0 < 0, R_1 > 0, R_2 < 0 \text{ and } \tau = \tau_1^*\}.$$

The saddle-node bifurcation reveals that if the releasing rate $\tau < \tau_1^*$, then there exist some parameter spaces such that the pests and natural enemies may coexist in the form of a positive equilibrium or a periodic orbit with a finite period for different initial values, and if the releasing rate $\tau > \tau_1^*$, then the pest population will be driven to extinction, as shown in Figure 4B,C.

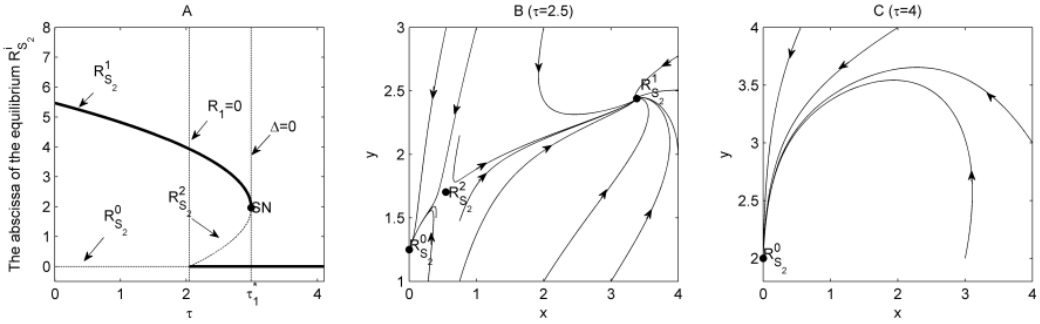

Figure 4. Bifurcation diagrams with respect to parameter τ, where SN denotes the saddle-node bifurcation, and the solid black curve indicates that the equilibrium is stable, otherwise it is unstable. The parameter values are fixed as follows: $K = 8$, $r = 3$, $\beta = 2$, $\delta_1 = 2$, $\omega = 1.55$, $\eta = 0.90$, $\alpha = 0.95$. B: $\tau = 2.5$. C: $\tau = 4$.

3.2.3. The Hopf bifurcation

For the characteristic equation related to the positive equilibrium $R^1_{S_2}(x_1, y_1)$ of system (3.1), we have

$$\lambda^2 + p_{R^1_{S_2}} \lambda + q_{R^1_{S_2}} = 0, \tag{3.15}$$

where

$$q_{R^1_{S_2}} = \frac{2rR_0x_1}{K(1+\omega x_1)}\left[\frac{KR_2}{2rR_0} - x_1\right] > 0. \tag{3.16}$$

and

$$p_{R^1_{S_2}} = \frac{1}{1+\omega x_1}\left[\frac{2r\omega}{K}x_1^2 - (\eta\beta - \delta_1\omega - \frac{r}{K} + r_1\omega)x_1 + \delta_1\right]. \tag{3.17}$$

Obviously, when $p_{R^1_{S_2}} = 0$, solving the characteristic equation (3.15), we can get two complex eigenvalues $\lambda_{1,2} = \pm ib_0$ with $b_0 = \sqrt{q_{R^1_{S_2}}}$. That is to say, the positive equilibrium $R^1_{S_2}$ is a center-type equilibrium of the linear system of system (3.1), which indicates that system (3.1) may undergo a Hopf bifurcation if the bifurcation parameters are chosen suitably.

We choose the releasing constant τ as the bifurcation parameter and fix all other parameters. To determine the critical bifurcation value τ^*, we consider the equation $p_{R^1_{S_2}}(\tau^*) = 0$, i.e.,

$$m_2(\tau^*)^2 + m_1\tau^* + m_0 = 0, \tag{3.18}$$

where $m_2 = \frac{16r^2\beta^2 a_4^2 R_0^2}{K^2}$, $m_1 = \frac{4r\beta R_0(2a_4a_6 - a_5^2 - 2r_1R_0 + \frac{2r\delta_1}{K})}{K}$, $m_0 = a_4^2[\frac{r\delta_1}{K} - r_1R_0]^4 + (2a_4a_6 - a_5^2)[\frac{r\delta_1}{K} - r_1R_0]^2$, $a_4 = \frac{K\omega}{2r\beta R_0^2}$, $a_5 = \frac{K}{2rR_0}(\frac{r_1\omega - \frac{r}{K} + \eta\beta - \delta_1\omega}{\beta} - \frac{r_1K}{r} - \frac{\delta_1}{R_0})$ and $a_6 = \frac{r\omega}{2\beta K}(\frac{r_1K}{r} + \frac{\delta_1}{R_0})^2 + \left[\frac{\delta_1}{\beta} - \frac{r_1\omega - \frac{r}{K} + \eta\beta - \delta_1\omega}{\beta}(\frac{r_1K}{2r} + \frac{\delta_1}{2R_0})\right]$. Denote $\Delta_3 \doteq m_1^2 - 4m_0m_2$, then for the existence of critical value τ^* we have the following results:

Lemma 3.2. The existence of parameter τ^* can be described as follows:

(i) if $\Delta_3 < 0$, then τ^* does not exist.

(ii) if $\Delta_3 = 0$ and $m_1 < 0$, then there exists a unique τ^*.

(iii) if $\Delta_3 > 0$, $m_0 = 0$ and $m_1 < 0$, then there exists a unique τ^*.

(V) if $\Delta_3 > 0$, $m_0 < 0$, then there exists a unique τ^*.

(IV) if $\Delta_3 > 0$, $m_0 > 0$ and $m_1 < 0$, then there exist two critical values of τ^*.

Based on Lemma 3.2, we assume that there exists at least a critical value τ^* such that $p_{R^1_{S_2}}(\tau^*) = 0$, and then address the Hopf bifurcation, i.e., we have the following main results:

Theorem 3.10. For system (3.1), assume that there exists a critical value $\tau^* > 0$ such that $p_{R^1_{S_2}}(\tau^*) = 0$, then system (3.1) undergoes a Hopf bifurcation and there is a unique limit cycle in the neighborhood of $R^1_{S_2}$ provided $R_4 > 1$.

Proof. Let $\lambda = a(\tau) + ib(\tau)$ be a complex root of the characteristic equation (3.15), where $a(\tau^*) = 0$ and $b(\tau^*) = b_0$. Substituting it into the characteristic equation (3.15), it becomes

$$[a(\tau) + ib(\tau)]^2 + p_{R^1_{S_2}}[a(\tau) + ib(\tau)] + q_{R^1_{S_2}} = 0,$$

which can be represented as

$$\begin{cases} a(\tau)^2 - b(\tau)^2 + p_{R^1_{S_2}}(\tau)a(\tau) + q_{R^1_{S_2}}(\tau) = 0, \\ 2a(\tau)b(\tau) + p_{R^1_{S_2}}(\tau)b(\tau) = 0. \end{cases} \tag{3.19}$$

Taking the partial derivative of (3.19) with respect to τ, we can obtain

$$\begin{cases} 2\left[a(\tau)a'(\tau) - b(\tau)b'(\tau)\right] + p_{R^1_{S_2}}(\tau)a'(\tau) + p'_{R^1_{S_2}}(\tau)a(\tau) + q'_{R^1_{S_2}}(\tau) = 0, \\ 2\left[a'(\tau)b(\tau) + a(\tau)b'(\tau)\right] + p'_{R^1_{S_2}}(\tau)b(\tau) + p_{R^1_{S_2}}(\tau)b'(\tau) = 0. \end{cases}$$

It follows from $a(\tau^*) = 0$, $p_{R^1_{S_2}}(\tau^*) = 0$ and $b(\tau^*) = b_0$ that we have

$$a'(\tau)|_{\tau=\tau^*} = -\frac{1}{2}p'_{R^1_{S_2}}(\tau)\Big|_{\tau=\tau^*}, \tag{3.20}$$

which is called the transversality condition [33, 34].

If $a'(\tau)|_{\tau=\tau^*} \neq 0$, then the transversality condition (3.20) is satisfied, which indicates that the Hopf bifurcation takes place and there exists a unique limit cycle in the neighborhood of the positive equilibrium $R^1_{S_2}$. By a simple calculation, we can obtain that

$$\begin{aligned} a'(\tau)|_{\tau=\tau^*} &= -\frac{1}{2(1+\omega x_1)}\left[\frac{4rw}{K}x_1 - (\eta\beta - \delta_1\omega - \frac{r}{K} + r_1\omega)\right]\frac{dx_1}{d\tau}\Big|_{\tau=\tau^*} \\ &= -\frac{2r\omega}{K(1+\omega x_1)}\left[(x_1 - \frac{K(\eta\beta - \delta_1\omega - \frac{r}{K} + r_1\omega)}{4r\omega}\right]\frac{dx_1}{d\tau}\Big|_{\tau=\tau^*}, \end{aligned} \tag{3.21}$$

where $\frac{dx_1}{d\tau}\Big|_{\tau=\tau^*} = -\frac{\beta}{\sqrt{R_2^2 + \frac{4rR_0R_1}{K}}} < 0$.

It follows from $p_{R^1_{S_2}} = \frac{1}{1+\omega x_1}\left[\frac{2r\omega}{K}x_1^2 - (\eta\beta - \delta_1\omega - \frac{r}{K} + r_1\omega)x_1 + \delta_1\right]$ that x_1 is a positive real root of the following equation:

$$\frac{2r\omega}{K}x_1^2 - (\eta\beta - \delta_1\omega - \frac{r}{K} + r_1\omega)x_1 + \delta_1 = 0 \tag{3.22}$$

at $\tau = \tau^*$, which indicates that

$$\Delta_4 \doteq (\eta\beta - \delta_1\omega - \frac{r}{K} + r_1\omega)^2 - \frac{8r\omega\delta_1}{K} \geq 0 \text{ and } \eta\beta - \delta_1\omega - \frac{r}{K} + r_1\omega > 0$$

in the above equation. Solving equation (3.22) yields two roots, denoted by

$$x_{11} = \frac{K(\eta\beta - \delta_1\omega - \frac{r}{K} + r_1\omega)}{4r\omega} + \frac{K\sqrt{\Delta_4}}{4r\omega} \text{ and } x_{12} = \frac{K(\eta\beta - \delta_1\omega - \frac{r}{K} + r_1\omega)}{4r\omega} - \frac{K\sqrt{\Delta_4}}{4r\omega}.$$

If $x_1 = x_{11}$, then we have

$$a'(\tau)|_{\tau=\tau^*} = -\frac{K\sqrt{\Delta_4}}{4r\omega}\frac{dx_1}{d\tau}\Big|_{\tau=\tau^*}. \tag{3.23}$$

If $x_1 = x_{12}$, then we have

$$a'(\tau)|_{\tau=\tau^*} = \frac{K\sqrt{\Delta_4}}{4r\omega}\frac{dx_1}{d\tau}\Big|_{\tau=\tau^*}. \tag{3.24}$$

Therefore, it follows from (3.23) and (3.24) that if $\Delta_4 > 0$, which is equivalent to the inequality

$$\frac{(\eta\beta - \delta_1\omega - \frac{r}{K} + r_1\omega)\sqrt{2r\delta_1\omega K}}{4r\delta_1\omega} > 1, \text{ i.e., } R_4 > 1,$$

then $a'(\tau)|_{\tau=\tau^*} \neq 0$, and consequently the Hopf bifurcation takes place at $\tau = \tau^*$.

To determine the stability of the limit cycle and the direction of the Hopf bifurcation in this case, we need to compute the first Liapunov coefficient $l_1(\tau^*)$ [34,35] related to the positive equilibrium $R^1_{S_2}$. To do this, we translate the origin of the coordinates to the positive equilibrium $R^1_{S_2}$ of system (3.1) by the change of variables

$$\bar{x} = x - x_1, \quad \bar{y} = y - y_1,$$

rewrite $(\bar{x}, \bar{y})$ as (x,y) and expand the right-hand side of system (3.1) in a Taylor series about the origin, then we can obtain

$$\begin{cases} \dfrac{dx}{dt} = ax + by + a_{20}x^2 + 2a_{11}xy + a_{30}x^3 + a_{21}x^2y + R_1(x,y), \\ \dfrac{dy}{d\tau} = cx + dy + b_{20}x^2 + 2b_{11}xy + b_{30}x^3 + b_{21}x^2y + R_2(x,y), \end{cases} \tag{3.25}$$

where $a \doteq r_1 - \frac{2r}{K}x_1 - \frac{\beta y_1}{(1+\omega x_1)^2}$, $b \doteq -\frac{\beta x_1}{1+\omega x_1}$, $c \doteq \frac{\eta\beta y_1}{(1+\omega x_1)^2}$, $d \doteq -\delta_1 + \frac{\eta\beta x_1}{1+\omega x_1}$, $a_{20} \doteq -\frac{r}{K} + \frac{\beta\omega y_1}{(1+\omega x_1)^3}$, $a_{11} \doteq -\frac{\beta}{2(1+\omega x_1)^2}$, $b_{20} \doteq -\frac{\eta\beta\omega y_1}{(1+\omega x_1)^3}$, $b_{11} \doteq \frac{\eta\beta}{2(1+\omega x_1)^2}$, $a_{30} \doteq -\frac{\beta\omega^2 y_1}{(1+\omega x_1)^4}$, $a_{21} \doteq \frac{\beta\omega}{(1+\omega x_1)^3}$, $b_{30} \doteq \frac{\eta\beta\omega^2 y_1}{(1+\omega x_1)^4}$, $b_{21} \doteq -\frac{\eta\beta\omega}{(1+\omega x_1)^3}$, and $R_1(x,y)$ and $R_2(x,y)$ are C^∞ functions in (x,y) at least of the fourth order.

Therefore, by employing the formula of the first Liapunov number $l_1(\tau^*)$ at the origin of (3.25) in [34, 35], we have

$$\begin{aligned} l_1(\tau^*) &= -\frac{r\omega x_1^2}{K\beta b_0^3}\left[\left(\frac{r_1\delta_1}{\beta^2} - \frac{\tau}{\beta}\right) + \frac{r\omega(\eta\beta - \delta_1\omega)}{\beta^2 K}x_1^3 + \frac{\beta K}{2r\omega}\left(\frac{\delta_1}{\beta} - \frac{\eta\beta - \delta_1\omega}{\beta}x_1\right)\left(\frac{\delta_1(\eta\beta - \delta_1\omega)}{\beta^2 x_1} + \frac{r\delta_1\omega}{\beta^2 K}\right)\right] \\ &= -\frac{r\omega x_1^2}{K\beta^3 b_0^3}\left[-R_1 + \frac{r\omega R_0}{K}x_1^3 + \frac{K\delta_1 R_0}{2r\omega}\left(\frac{\delta_1}{R_0} - x_1\right)\left(\frac{R_0}{x_1} + \frac{r\omega}{K}\right)\right]. \end{aligned}$$

Moreover, if $l_1(\tau^*) < 0$, then system (3.1) undergoes a supercritical Hopf bifurcation at $\tau = \tau^*$ and there is a unique and stable limit cycle [35]. If $l_1(\tau^*) > 0$, then system (3.1) undergoes a subcritical Hopf bifurcation at $\tau = \tau^*$ and there is a unique and unstable limit cycle [35]. This completes the proof.

To confirm the main results obtained here, we choose τ as the bifurcation parameter and fix the others as those shown in Figure 5. Bifurcation diagrams shown in Figure 5A,B indicate there exist Hopf bifurcation points τ_i^* $(i = 2, 3, 4)$ marked as HB. Moreover, by a simple calculation, we have $\tau_4^* = 0.27$, $p_{R^1_{S_2}}(\tau_4^*) = 0$, $a'_{R^1_{S_2}}(\tau)|_{\tau=\tau_4^*} \neq 0$ and $l_1(\tau_4^*) < 0$, i.e., system (3.1) undergoes a supercritical Hopf bifurcation at τ_4^* and it has a stable limit cycle in the neighborhood of $R^1_{S_2}$, as shown in Figure 5B,C.

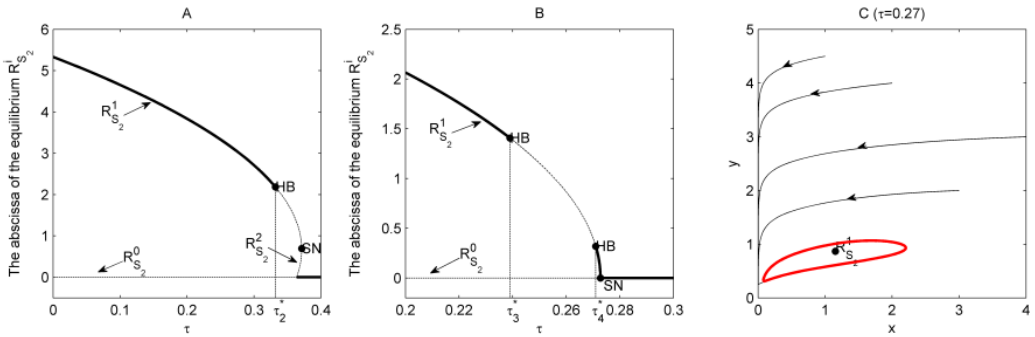

Figure 5. Bifurcation diagrams with respect to parameter τ, where *HB* denotes the Hopf bifurcation and *SN* represents the saddle-node bifurcation, and the solid black curve indicates that the equilibrium is stable, otherwise it is unstable. The parameter values are fixed as follows: $K = 8$, $r = 3$, $\beta = 5.5$, $\delta_1 = 1$, $\omega = 3$, $\eta = 0.5$. A: $\alpha = 1.0$. B: $\alpha = 1.5$. C: $\alpha = 1.5$, $\tau = 0.27$.

3.2.4. The Bogdanov-Takens bifurcation

From Lemma 3.1 and Theorem 3.6, we can obtain that if $R_0 < 0$, $R_1 > 0$, $R_2 < 0$ and $\Delta = 0$, then $R^1_{S_2}$ collides with $R^2_{S_2}$ as shown in Figure 4-A, and for convenience we still denote it by $R^1_{S_2}$. According to the characteristic equation (3.7), by a simple calculation, we have

$$\begin{cases} p_{R^1_{S_2}} = \dfrac{1}{1+\omega x_1}\left[\dfrac{2rw}{K}x_1^2 - (\eta\beta - \delta_1\omega - \dfrac{r}{K} + r_1\omega)x_1 + \delta_1\right], \\ q_{R^1_{S_2}} = \dfrac{2rR_0x_1}{K(1+\omega x_1)}\left[\dfrac{KR_2}{2rR_0} - x_1\right] \end{cases} \tag{3.26}$$

with $x_1 = \frac{r_1K}{2r} + \frac{\delta_1}{2(\eta\beta-\delta_1\omega)} = \frac{KR_2}{2rR_0}$. Note that we have $q_{R^1_{S_2}} = 0$ in this case. And if $p_{R^1_{S_2}} = 0$ (i.e.,$R_3 = 1$), then the characteristic equation (3.7) related to the positive equilibrium $R^1_{S_2}$ has two zero eigenvalues. This suggests that system (3.1) may admit a Bogdanov-Takens bifurcation [30, 31, 34] under a small parameter perturbation if the bifurcation parameters are chosen suitably and we confirm this by giving the following theorem.

Theorem 3.11. Suppose $p_{R^1_{S_2}} = 0$ and $q_{R^1_{S_2}} = 0$, then the positive equilibrium $R^1_{S_2}(x_1, y_1)$ of system (3.1) is a cusp of codimension 2 if $ef \neq 0$, where $e = 2b_{11}+2a_{20}-\frac{2aa_{11}}{b}$ and $f = aa_{20}-\frac{2a^2a_{11}}{b}+bb_{20}-2ab_{11}$.

Proof. Assume that $p_{R^1_{S_2}} = 0$ and $q_{R^1_{S_2}} = 0$, translating the positive equilibrium $R^1_{S_2}(x_1, y_1)$ to the origin by the change of variables $u = x - x_1$ and $v = y - y_1$, renaming (u, v) as (x, y) and expanding the right-hand side of system (3.1) in a Taylor series about the origin, then we can obtain

$$\begin{cases} \dfrac{dx}{dt} = ax + by + a_{20}x^2 + 2a_{11}xy + R_3(x, y), \\ \dfrac{dy}{dt} = cx + dy + b_{20}x^2 + 2b_{11}xy + R_4(x, y), \end{cases} \tag{3.27}$$

where $R_3(x, y)$ and $R_4(x, y)$ are C^∞ functions in (x, y) at least of the third order.

Notice that $b \neq 0$, making the following change of variables

$$u = x, \quad v = ax + by$$

and renaming (u, v) as (x, y), then system (3.27) becomes

$$\begin{cases} \dfrac{dx}{dt} = y + (a_{20} - \dfrac{2aa_{11}}{b})x^2 + \dfrac{2a_{11}}{b}xy + R_5(x, y), \\ \dfrac{dy}{dt} = (aa_{20} - \dfrac{2a^2a_{11}}{b} + bb_{20} - 2ab_{11})x^2 + (\dfrac{2aa_{11}}{b} + 2b_{11})xy + R_6(x, y), \end{cases} \tag{3.28}$$

where $R_5(x, y)$ and $R_6(x, y)$ are C^∞ functions in (x, y) at least of the third order. Let

$$u = x - \frac{a_{11}}{b}x^2, \quad v = y + (a_{20} - \frac{2aa_{11}}{b})x^2$$

and rename (u, v) as (x, y), then system (3.28) can be written as

$$\begin{cases} \dfrac{dx}{dt} = y + R_7(x, y), \\ \dfrac{dy}{dt} = (aa_{20} - \dfrac{2a^2a_{11}}{b} + bb_{20} - 2ab_{11})x^2 + (2b_{11} + 2a_{20} - \dfrac{2aa_{11}}{b})xy + R_8(x, y), \end{cases} \tag{3.29}$$

which can be represented as

$$\begin{cases} \dfrac{dx}{dt} = y + R_7(x,y), \\ \dfrac{dy}{dt} = exy + fx^2 + R_8(x,y), \end{cases}$$

where $e = 2b_{11} + 2a_{20} - \frac{2aa_{11}}{b}$ and $f = aa_{20} - \frac{2a^2a_{11}}{b} + bb_{20} - 2ab_{11}$, and $R_7(x,y)$ and $R_8(x,y)$ are C^∞ functions in (x,y) at least of the third order.

Therefore, if $ef \neq 0$, then the positive equilibrium $R^1_{S_2}$ of system (3.1) is a cusp of codimension 2 by the qualitative theory of ordinary differential equations and the theory of differential manifolds [30,34]. This completes the proof.

Further, we choose τ and δ_1 as bifurcation parameters, and suppose that there exist parameters $\tau^* > 0$ and $\delta_1^* > 0$ such that $p_{R^1_{S_2}} = 0$ and $q_{R^1_{S_2}} = 0$, i.e.,

$$\begin{cases} \dfrac{2r\omega}{K}\left[\dfrac{r\delta_1^* + Kr_1(\eta\beta - \delta_1^*\omega)}{2r(\eta\beta - \delta_1^*\omega)}\right]^2 - (\eta\beta - \delta_1^*\omega - \dfrac{r}{K} + r_1\omega)\left[\dfrac{r\delta_1^* + Kr_1(\eta\beta - \delta_1^*\omega)}{2r(\eta\beta - \delta_1^*\omega)}\right] + \delta_1^* = 0, \\ \dfrac{4r}{K}(\beta\tau^* - r_1\delta_1^*)(\eta\beta - \delta_1^*\omega) + \left[r_1(\eta\beta - \delta_1^*\omega) + \dfrac{r\delta_1^*}{K}\right]^2 = 0. \end{cases}$$

Note that the existence of (τ^*, δ_1^*) can be easily confirmed by numerical investigations. We study the dynamical behavior of system (3.1) when parameters τ and δ_1 vary in a small neighborhood of (τ^*, δ_1^*), and analyze the local representations of the bifurcation curves in a small neighborhood of the positive equilibrium $R^1_{S_2}$.

Theorem 3.12. Suppose $ef \neq 0$ at the positive equilibrium $R^1_{S_2}$, then system (3.1) undergoes a Bogdanov-Takens bifurcation in a small neighborhood of $R^1_{S_2}$ as (τ, δ_1) varies near (τ^*, δ_1^*) provided that $ae + 2f \neq 0$, and system (3.1) has the following bifurcation behaviors in a small neighborhood of $R^1_{S_2}$:

(i) the saddle-node bifurcation curve: $SN = \{(\varepsilon_1, \varepsilon_2) | \ \frac{ge^4}{f_1^3} = 0\}$;

(ii) the Hopf bifurcation curve: $HB = \{(\varepsilon_1, \varepsilon_2) | \ \frac{ge^4}{f_1^3} + \frac{h^2e^4}{f_1^4} = 0, \frac{he^2}{f_1^2} > 0\}$;

(iii) the homoclinic bifurcation curve: $HL = \{(\varepsilon_1, \varepsilon_2) | \ \frac{ge^4}{f_1^3} + \frac{49}{25}\frac{h^2e^4}{f_1^4} = 0, \frac{he^2}{f_1^2} > 0\}$.

Proof. First of all, let $\delta_1 = \delta_1^* - \varepsilon_1$ and $\tau = \tau^* - \varepsilon_2$, then system (3.1) can be represented as

$$\begin{cases} \dfrac{dx}{dt} = r_1 x - \dfrac{r}{K}x^2 - \dfrac{\beta xy}{1 + \omega x}, \\ \dfrac{dy}{dt} = \dfrac{\eta\beta xy}{1 + \omega x} - (\delta_1^* - \varepsilon_1)y + (\tau^* - \varepsilon_2). \end{cases} \tag{3.30}$$

Translating the positive equilibrium $R^1_{S_2}(x_1, y_1)$ to the origin by the change of variables $\bar{x} = x - x_1$ and $\bar{y} = y - y_1$, renaming $(\bar{x}, \bar{y})$ as (x, y) and expanding the right-hand side of system (3.30) in a Taylor series about the origin, then we can obtain

$$\begin{cases} \dfrac{dx}{dt} = ax + by + a_{20}x^2 + 2a_{11}xy + R_9(x, y, \varepsilon_1, \varepsilon_2), \\ \dfrac{dy}{dt} = (\varepsilon_1 y_1 - \varepsilon_2) + cx + d_1 y + b_{20}x^2 + 2b_{11}xy + R_{10}(x, y, \varepsilon_1, \varepsilon_2), \end{cases} \tag{3.31}$$

where $d_1 = (-\delta_1^* + \varepsilon_1) + \frac{\eta\beta x_1}{1+\omega x_1}$, and $R_9(x, y, \varepsilon_1, \varepsilon_2)$ and $R_{10}(x, y, \varepsilon_1, \varepsilon_2)$ are C^∞ functions in (x, y) at least of the third order, whose coefficients depend smoothly on ε_1 and ε_2. Let

$$u = x, \quad v = ax + by$$

and rename (u, v) as (x, y), then system (3.31) can be written as

$$\begin{cases} \dfrac{dx}{dt} = y + (a_{20} - \dfrac{2aa_{11}}{b})x^2 + \dfrac{2a_{11}}{b}xy + R_{11}(x, y, \varepsilon_1, \varepsilon_2), \\ \dfrac{dy}{dt} = b(\varepsilon_1 y_1 - \varepsilon_2) - a\varepsilon_1 x + \varepsilon_1 y + (aa_{20} - \dfrac{2a^2a_{11}}{b} + bb_{20} - 2ab_{11})x^2 + (\dfrac{2aa_{11}}{b} + 2b_{11})xy + R_{12}(x, y, \varepsilon_1, \varepsilon_2), \end{cases} \tag{3.32}$$

where $R_{11}(x, y, \varepsilon_1, \varepsilon_2)$ and $R_{12}(x, y, \varepsilon_1, \varepsilon_2)$ are C^∞ functions in (x, y) at least of the third order, whose coefficients depend smoothly on ε_1 and ε_2. Making the following change of variables

$$u = x - \frac{a_{11}}{b}x^2, \quad v = y + (a_{20} - \frac{2aa_{11}}{b})x^2$$

and renaming (u, v) as (x, y), then system (3.32) becomes

$$\begin{cases} \dfrac{dx}{dt} = y + R_{13}(x, y, \varepsilon_1, \varepsilon_2), \\ \dfrac{dy}{dt} = b(\varepsilon_1 y_1 - \varepsilon_2) - a\varepsilon_1 x + \varepsilon_1 y + exy + f_1 x^2 + R_{14}(x, y, \varepsilon_1, \varepsilon_2), \end{cases} \tag{3.33}$$

where $f_1 = aa_{20} - \frac{2a^2a_{11}}{b} + bb_{20} - 2ab_{11} - \frac{aa_{11}}{b}\varepsilon_1 - \varepsilon_1(a_{20} - \frac{2aa_{11}}{b})$, and $R_{13}(x, y, \varepsilon_1, \varepsilon_2)$ and $R_{14}(x, y, \varepsilon_1, \varepsilon_2)$ are C^∞ functions in (x, y) at least of the third order, whose coefficients depend smoothly on ε_1 and ε_2.

Next, we make the following change of variables

$$u = x, \quad y = y + R_{13}(x, y, \varepsilon_1, \varepsilon_2)$$

and rename (u, v) as (x, y), then system (3.33) becomes

$$\begin{cases} \dfrac{dx}{dt} = y, \\ \dfrac{dy}{dt} = b(\varepsilon_1 y_1 - \varepsilon_2) - a\varepsilon_1 x + \varepsilon_1 y + exy + f_1 x^2 + R_{15}(x, y, \varepsilon_1, \varepsilon_2), \end{cases} \tag{3.34}$$

where $R_{15}(x, y, \varepsilon_1, \varepsilon_2)$ is a C^∞ function in (x, y) at least of the third order, whose coefficients depend smoothly on ε_1 and ε_2. By setting $u = x + \frac{\varepsilon_1}{e}$ and $v = y$, renaming (u, v) as (x, y), then system (3.34) becomes

$$\begin{cases} \dfrac{dx}{dt} = y, \\ \dfrac{dy}{dt} = g + hx + exy + f_1 x^2 + R_{16}(x, y, \varepsilon_1, \varepsilon_2), \end{cases} \tag{3.35}$$

where $g = b(\varepsilon_1 y_1 - \varepsilon_2) + \frac{f_1\varepsilon_1^2}{e^2} + \frac{a\varepsilon_1^2}{e}$ and $h = -a\varepsilon_1 - \frac{2f_1\varepsilon_1}{e}$, and $R_{14}(x, y, \varepsilon_1, \varepsilon_2)$ is a C^∞ function in (x, y) at least of the third order, whose coefficients depend smoothly on ε_1 and ε_2. Moreover,

$$\lim_{\varepsilon_j \to 0} f_1 = aa_{20} - \frac{2a^2a_{11}}{b} + bb_{20} - 2ab_{11} = f,$$

where $j = 1, 2$.

Notice that $f_1 \neq 0$ when ε_j are small. Making the change of variables one more time by setting

$$u = \frac{e^2}{f_1}x, \ \ v = \frac{e^3}{f_1^2}y, \ \ \tau = \frac{e}{f_1}t$$

when ε_j are small, and renaming (u, v, τ) as (x, y, t), then system (3.35) can be represented as

$$\begin{cases} \dfrac{dx}{dt} = y, \\ \dfrac{dy}{dt} = \mu_1(\varepsilon_1, \varepsilon_2) + \mu_2(\varepsilon_1, \varepsilon_2)x + xy + x^2 + R_{17}(x, y, \varepsilon_1, \varepsilon_2), \end{cases} \tag{3.36}$$

where $\mu_1(\varepsilon_1, \varepsilon_2) = \frac{ge^4}{f_1^3}$ and $\mu_2(\varepsilon_1, \varepsilon_2) = \frac{he^2}{f_1^2}$, and $R_{15}(x, y, \varepsilon_1, \varepsilon_2)$ is a C^∞ function in (x, y) at least of the third order, whose coefficients depend smoothly on ε_1 and ε_2. Moreover, by a simple calculation, we can obtain that

$$\left|\frac{\partial(\mu_1(\varepsilon_1, \varepsilon_2), \mu_2(\varepsilon_1, \varepsilon_2))}{\partial(\varepsilon_1, \varepsilon_2)}\right|_{(0,0)} = (-1)\frac{be^5}{f^5}(ae + 2f),$$

when $ae + 2f \neq 0$, the above parameter transformation is a homeomorphism in a small neighborhood of the origin [36], and μ_1 and μ_2 are independent parameters.

Based on the above analyses, according to the theorems in Bogdanov and Takens [30, 31], we can obtain the local representations of the bifurcation curves of system (3.36) in a small neighborhood of the origin if $ae + 2f \neq 0$, and it is equivalent to the bifurcation behavior of system (3.1) in a small neighborhood of $R^1_{S_2}$, as shown in Theorem 3.12. This completes the proof.

4. The analysis of non-smooth Filippov system (2.2)

In this section, we mainly analyze the complete behavior of non-smooth Filippov system (2.2) including the existence, stability of the regular/virtual equilibria, pseudo-equilibria, sliding segments, sliding bifurcations and sliding periodic solutions.

4.1. The analysis of the sliding segments and tangent points

In order to analyze the dynamical behavior of non-smooth Filippov system (2.2) in R^2_+, we need to analyze the existence and stability of the sliding segments and tangent points firstly.

The sliding segment: by a simple calculation, we can obtain

$$\begin{aligned} \sigma(x, y) &= \langle H_X(x, y), f_1(x, y)\rangle\langle H_X(x, y), f_2(x, y)\rangle \\ &= \langle (1, 0), (rx - \frac{r}{K}x^2 - \frac{\beta xy}{1 + \omega x}, \frac{\eta\beta xy}{1 + \omega x} - \delta y)\rangle \\ &\ \ \langle (1, 0), (rx - \frac{r}{K}x^2 - \frac{\beta xy}{1 + \omega x} - \alpha x, \frac{\eta\beta xy}{1 + \omega x} - \delta_1 y + \tau)\rangle \\ &= x^2\left(r - \frac{r}{K}x - \frac{\beta y}{1 + \omega x}\right)\left(r_1 - \frac{r}{K}x - \frac{\beta y}{1 + \omega x}\right), \end{aligned}$$

where $r_1 = r - \alpha$ and $0 < ET < K$. It is easy to obtain that if $x = ET$, then $\sigma(x, y) \leq 0$ is equivalent to the inequalities

$$\frac{r_1}{\beta} + (\frac{r_1\omega}{\beta} - \frac{r}{\beta K})ET - \frac{r\omega}{\beta K}ET^2 \leq y \leq \frac{r}{\beta} + (\frac{r\omega}{\beta} - \frac{r}{\beta K})ET - \frac{r\omega}{\beta K}ET^2.$$

For convenience, denote

$$y_{\min} \doteq \frac{r_1}{\beta} + (\frac{r_1\omega}{\beta} - \frac{r}{\beta K})ET - \frac{r\omega}{\beta K}ET^2,$$
$$y_{\max} \doteq \frac{r}{\beta} + (\frac{r\omega}{\beta} - \frac{r}{\beta K})ET - \frac{r\omega}{\beta K}ET^2,$$

where $y_{\min} \geq 0$ for all $ET \in (0, \frac{r_1 K}{r}]$; $y_{\max} > 0$ for all $ET \in (0, K)$. And if one of the following conditions

$$y < y_{\min} \quad \text{or} \quad y > y_{\max}$$

holds true, then $\sigma(x, y) > 0$.

Therefore, the sliding segment of non-smooth Filippov system (2.2) is defined as

$$\Sigma_s = \{(x, y) | x = ET, \max\{0, y_{\min}\} \leq y \leq y_{\max}\},$$

and the crossing set is given as

$$\Sigma_c = \{(x, y) | x = ET, 0 \leq y < \max\{0, y_{\min}\} \quad \text{or} \quad y > y_{\max}\}.$$

Moreover, we have

$$\begin{aligned}\langle H_X(x, y), f_1(x, y)\rangle &= \langle (1, 0), (rx - \frac{r}{K}x^2 - \frac{\beta xy}{1 + \omega x}, \frac{\eta\beta xy}{1 + \omega x} - \delta y)\rangle \\ &= rx - \frac{r}{K}x^2 - \frac{\beta xy}{1 + \omega x} > 0\end{aligned}$$

and

$$\begin{aligned}\langle H_X(x, y), f_2(x, y)\rangle &= \langle (1, 0), (rx - \frac{r}{K}x^2 - \frac{\beta xy}{1 + \omega x} - \alpha x, \frac{\eta\beta xy}{1 + \omega x} - \delta_1 y + \tau)\rangle \\ &= r_1 x - \frac{r}{K}x^2 - \frac{\beta xy}{1 + \omega x} < 0\end{aligned}$$

for all points $(x, y) \in \Sigma_s$, which indicates that the sliding segment Σ_s is stable.

According to the Filippov convex method [32], we can obtain the following sliding dynamical equation defined in $(x, y) \in \Sigma_s$

$$\frac{dy}{dt} = \lambda(\frac{\eta\beta x}{1 + \omega x}y - \delta y) + (1 - \lambda)(\frac{\eta\beta x}{1 + \omega x}y - \delta_1 y + \tau) \doteq F(y), \ x(t) = ET, \tag{4.1}$$

where

$$\lambda = \frac{\langle (1, 0), ((r_1 - \frac{rx}{K})x - \frac{\beta x}{1+\omega x}y, \frac{\eta\beta x}{1+\omega x}y - \delta_1 y + \tau)\rangle}{\langle (1, 0), (-\alpha x, (\delta - \delta_1)y + \tau)\rangle} = (1 - \frac{r}{\alpha}) + \frac{rET}{\alpha K} + \frac{\beta y}{\alpha(1 + \omega ET)}.$$

The equilibrium $R_0(x^*, y^*) \in \Sigma_s$ of system (4.1) is called the pseudo-equilibrium of non-smooth Filippov system (2.2).

Tangent point: The tangent points $T_i(x_i, y_i)(i = 1, 2)$ of non-smooth Filippov system (2.2) satisfy the following equations

$$\begin{cases} H(x_i, y_i) = 0, \\ \langle H_X(x_i, y_i), f_i(x_i, y_i)\rangle = 0. \end{cases}$$

By a simple calculation, we have

$$\begin{cases} x_1 = ET, \quad y_1 = y_{\max}; \\ x_2 = ET, \quad y_2 = y_{\min}. \end{cases}$$

That is to say, the sliding segment Σ_s is delimited by tangent points $T_1(x_1, y_1)$ and $T_2(x_2, y_2)$, which lie between the horizontal non-zero isocline $L^1_{S_1}$ of subsystem S_1 and $L^1_{S_2}$ of subsystem S_2, as shown in Figure 6A. Note that the tangent point T_2 becomes an end point of sliding segment once $y_{\min}$ is less than zero. Therefore, we call $T_2(ET, y_{\min}) \in R^2_+$ as a tangent point if $ET \in (0, \frac{r_1 K}{r}]$. Otherwise, if $ET \in (\frac{r_1 K}{r}, K)$, we call T_2 as an end point of the sliding segment Σ_s.

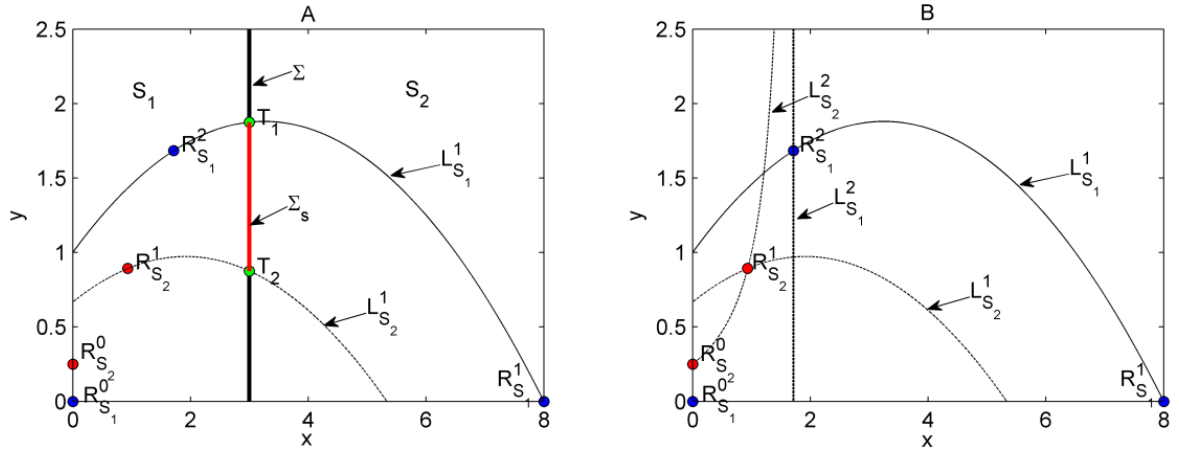

Figure 6. The sliding segment Σ_s, tangent points and the distribution of equilibria of non-smooth Filippov system (2.2), where $L^1_{S_1}$ and $L^2_{S_1}$ are non-zero isoclines of subsystem S_1; $L^1_{S_2}$ and $L^2_{S_2}$ are non-zero isoclines of subsystem S_2. The parameter values are fixed as follows: $K = 8, r = 3, \beta = 3, \delta = \delta_1 = 2, \omega = 2/3, \eta = 5/6, \tau = 1/2, \alpha = 1$ and $ET = 3$.

4.2. Equilibria of non-smooth Filippov system (2.2)

For the equilibria of non-smooth Filippov system (2.2), there are four types: regular equilibrium, virtual equilibrium, pseudo-equilibrium and boundary equilibrium, which are associated with the discontinuity boundary Σ and have been defined in Section 2. For convenience, the equilibria of subsystem S_1 are denoted by $R^i_{S_1}(x^i_{S_1}, y^i_{S_1})$ and the equilibria of subsystem S_2 are denoted by $R^i_{S_2}(x^i_{S_2}, y^i_{S_2})$, $i = 0, 1, 2$.

For the existence and stability of the pseudo-equilibrium $R_0(x^*, y^*)$ of non-smooth Filippov system (2.2), we only need to consider the existence and stability of equilibrium of system (4.1). Thus, we consider the equation $F(y) = 0$, i.e.,

$$\lambda\left(\frac{\eta\beta ET}{1 + \omega ET}y - \delta y\right) + (1 - \lambda)\left(\frac{\eta\beta ET}{1 + \omega ET}y - \delta_1 y + \tau\right) = 0, \tag{4.2}$$

which can be represented as

$$\frac{\beta(\delta_1-\delta)}{\alpha(1+\omega ET)}y^2+\left[-\delta-(\frac{r}{\alpha}-\frac{rET}{\alpha K})(\delta_1-\delta)+\frac{\eta\beta ET}{1+\omega ET}-\frac{\beta\tau}{\alpha(1+\omega ET)}\right]y+\frac{r\tau}{\alpha}\left(1-\frac{ET}{K}\right)=0. \quad (4.3)$$

If $\delta_1=\delta$ (i.e., the pesticide does not affect the predator), solving the above equation with respect to y, we can obtain

$$y^*=\frac{\frac{\tau r}{\alpha}(\frac{ET}{K}-1)}{\frac{\eta\beta ET}{1+\omega ET}-\frac{\beta\tau}{\alpha(1+\omega ET)}-\delta},$$

where $y^*\in[max\{0,y_{\min}\},y_{\max}]$ if and only if $ET\in[x^1_{S_2},x^2_{S_1}]$. Moreover, it is easy to obtain that

$$F'(y^*)=-\frac{\beta\tau}{\alpha(1+\omega ET)}+\frac{\eta\beta ET}{1+\omega ET}-\delta=-\frac{\tau r}{\alpha y^*}(1-\frac{ET}{K})<0,$$

which indicates that the pseudo-equilibrium $R_0(x^*,y^*)=R_0(ET,y^*)\in\Sigma_s$ is locally stable. Further, we have the following result.

Lemma 4.1. Suppose $\delta_1=\delta$, then non-smooth Filippov system (2.2) has a unique and stable pseudo-equilibrium $R_0(ET,y^*)$ if and only if $ET\in[x^1_{S_2},x^2_{S_1}]$.

If $\delta_1>\delta$, it is clear that Eq (4.3) have at most two positive real roots:

$$y_1^*=\frac{(r-\frac{rET}{K})(1+\omega ET)}{2\beta}+\frac{\alpha\delta+\beta\tau-\alpha(\eta\beta-\delta\omega)ET}{2\beta(\delta_1-\delta)}+\frac{\alpha(1+\omega ET)\sqrt{\Delta_5}}{2\beta(\delta_1-\delta)}$$

and

$$y_2^*=\frac{(r-\frac{rET}{K})(1+\omega ET)}{2\beta}+\frac{\alpha\delta+\beta\tau-\alpha(\eta\beta-\delta\omega)ET}{2\beta(\delta_1-\delta)}-\frac{\alpha(1+\omega ET)\sqrt{\Delta_5}}{2\beta(\delta_1-\delta)},$$

where

$$\Delta_5\doteq\left[-\delta-(\frac{r}{\alpha}-\frac{rET}{\alpha K})(\delta_1-\delta)+\frac{\eta\beta ET}{1+\omega ET}-\frac{\beta\tau}{\alpha(1+\omega ET)}\right]^2-4\frac{\beta r\tau(\delta_1-\delta)(1-\frac{ET}{K})}{\alpha^2(1+\omega ET)}>0. \quad (4.4)$$

This indicates that there may exist two pseudo-equilibria, denoted by $R_0^1(ET,y_1^*)$ and $R_0^2(ET,y_2^*)$, as shown in Figure 7. Further, by a simple calculation, we can obtain that if $\max\{0,y_{\min}\}\le y_2^*<y_1^*\le y_{\max}$, system (2.2) can exactly exist two pseudo-equilibria, and

$$F'(y_1^*)=\sqrt{\Delta_5}\quad\text{and}\quad F'(y_2^*)=-\sqrt{\Delta_5},$$

which indicate that $R_0^1(ET,y_1^*)$ is unstable provided that it lies in the Σ_s, and $R_0^2(ET,y_2^*)$ is locally stable provided that it lies in the Σ_s.

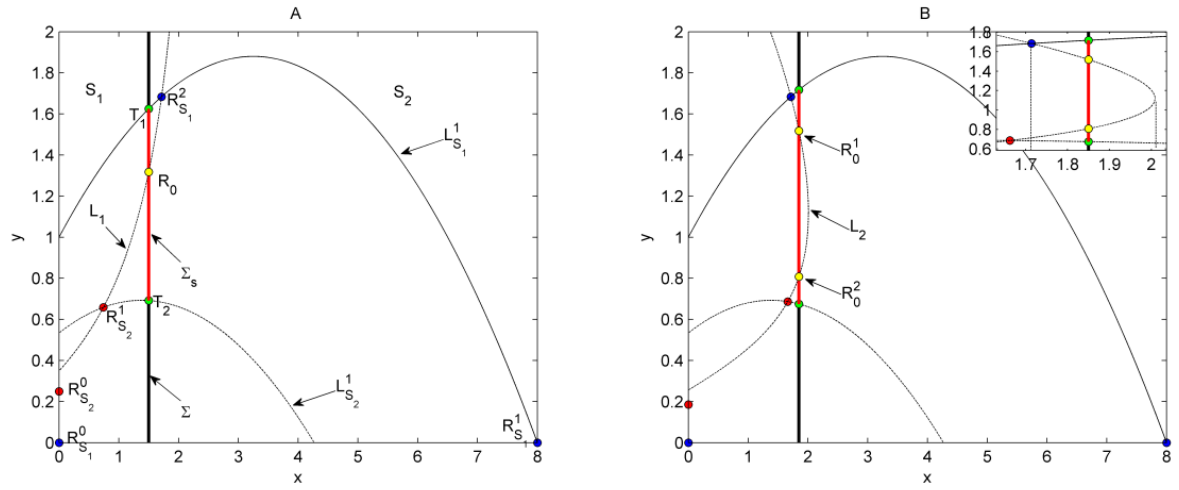

Figure 7. Illustrations of the existence of the pseudo-equilibria, where the parameter values are fixed as follows: $K = 8$, $r = 3$, $\beta = 3$, $\omega = 2/3$, $\eta = 5/6$, $\tau = 1/2$, $\alpha = 1.4$. A: $ET = 1.5$, $\delta_1 = \delta = 2$. B: $ET = 1.85$, $\delta_1 = 2.7$, $\delta = 2$.

Note that to show how the threshold value ET affects the existence of pseudo-equilibria of system (2.2), we first consider the function $F(y)$ defined in (4.1) as a function of x, i.e., the curve L_1 or L_2 shown in Figure 7, which can intersect with isoclines $L^1_{S_1}$ and $L^1_{S_2}$ at two points $R^1_{S_2}$ and $R^2_{S_1}$. Therefore, the horizontal components of both points may confirm the ranges of ET, within them system (2.2) could exist one or two pseudo-equilibria, as shown in Figure 7. In particular, if $\delta_1 = \delta$, then there exists a pseudo-equilibrium $R_0(ET, y^*) \in \Sigma_s$ with $ET \in [x^1_{S_2}, x^2_{S_1}]$. If $\delta_1 > \delta$, then for $ET \in [x^1_{S_2}, x^2_{S_1})$, there exists a unique pseudo-equilibrium R^1_0; for $ET \in [x^2_{S_1}, ET_1)$ with $\Delta_5(ET_1) = 0$ (here Δ_5 is considered as a function of ET defined by (4.4)), there exist two pseudo-equilibria R^1_0 and R^2_0, shown in Figure 7B. Especially, if $ET = ET_1$, then R^1_0 collides with R^2_0.

Based on the above analyses, we can now clarify the types of equilibria of non-smooth Filippov system (2.2). It follows from the conditions of existence and stability of equilibria of subsystem S_1, as shown in Section 2, then we consider the following three cases:

$$(C_1): 0 < \frac{\delta}{\eta\beta - \delta\omega} < K;\ (C_2): \frac{\delta}{\eta\beta - \delta\omega} < 0;\ (C_3): \frac{\delta}{\eta\beta - \delta\omega} \geq K.$$

For Case (C_1), according to the properties of subsystem S_2, we obtain that if $R_0 > 0$ and $R_1 < 0$, then there exist two equilibria: a boundary equilibrium $R^0_{S_2}(0, \frac{\tau}{\delta_1})$ which is a unstable saddle, and a positive equilibrium $R^1_{S_2}(x^1_{S_2}, y^1_{S_2})$ with

$$x^1_{S_2} = \frac{KR_2 - K\sqrt{R_2^2 + \frac{4rR_0R_1}{K}}}{2rR_0},\ y^1_{S_2} = (r_1 - \frac{r}{K}x^1_{S_2})\frac{1 + \omega x^1_{S_2}}{\beta}.$$

While subsystem S_1 has a unique positive equilibrium $R^2_{S_1}(\frac{\delta}{\eta\beta - \delta\omega}, \frac{r\eta(K\eta\beta - K\delta\omega - \delta)}{K(\eta\beta - \delta\omega)^2})$.

If $\delta_1 = \delta$, by a simple calculation, we obtain that $x^1_{S_2} < \frac{\delta}{\eta\beta - \delta\omega}$, which indicates that $R^1_{S_2}$ is on the left of $R^2_{S_1}$, as shown in Figure 6B and Figure 7A. And from Figure 7A, it is easy to see that $R^0_{S_1}$ is always

a regular equilibrium for subsystem S_1, $R^1_{S_1}$ is always a virtual equilibrium for subsystem S_1 and $R^0_{S_2}$ is always a virtual equilibrium for subsystem S_2. Further, the existence of all types of equilibria will be discussed briefly in the following:

(i) If $0 < ET < x^1_{S_2}$, we conclude that $R^2_{S_1}$ is a virtual equilibrium for subsystem S_1, $R^1_{S_2}$ is a regular equilibrium for subsystem S_2, and T_1 is an invisible tangent point and T_2 is a visible tangent point [23, 24].

(ii) If $x^1_{S_2} < ET < x^2_{S_1}$, we have that $R^2_{S_1}$ is a virtual equilibrium for subsystem S_1, $R^1_{S_2}$ becomes a virtual equilibrium for subsystem S_2, and T_1 is an invisible tangent point and T_2 becomes an invisible tangent point. Moreover, there exists a pseudo-equilibrium R_0.

(iii) If $x^2_{S_1} < ET < K$, then R_0 disappears, $R^2_{S_1}$ becomes a regular equilibrium for subsystem S_1, $R^1_{S_2}$ is a virtual equilibrium for subsystem S_2, T_1 becomes a visible tangent point and T_2 is an invisible tangent point. Especially, when $ET = x^1_{S_2}$ (or $ET = x^2_{S_1}$), $R^1_{S_2}$ (or $R^2_{S_1}$) collides with Σ, which is a boundary equilibrium. Moreover, three points T_2, $R^1_{S_2}$ and R_0 collide together in this case.

If $\delta_1 > \delta$, the position relations of all possible equilibria of two subsystems are hard to determine analytically. However, similar results can be obtained numerically as those shown above, so we omit them here. For Cases (C_2) and (C_3), subsystem S_1 only has steady state $R^0_{S_1}(0, 0)$ which is unstable, and exists a boundary equilibrium $R^1_{S_1}(K, 0)$ which is globally stable related to region S_1. The positive equilibria of subsystem S_2 lie between $R^0_{S_1}(0, 0)$ and $R^1_{S_1}(K, 0)$. Therefore, we can discuss the types of equilibria of system (2.2) similarly.

4.3. Local and global sliding bifurcation analyses

In this subsection, we address the bifurcations related to equilibria and sliding cycles concerning sliding segment Σ_s.

4.3.1. τ-bifurcations

Note that one of the main purposes of the present paper is to address the integrated pest management strategies for pest control and propose the non-smooth Filippov system (2.2), which indicates that how the key parameters related to control effectiveness affect the dynamics of system (2.2) are quite important. Thus, in this section we choose the releasing constant τ as a bifurcation parameter and fix all others to discuss the variations of the trajectories and equilibria of system (2.2).

For Case (C_1), if $\delta_1 = \delta$, there may exist a stable pseudo-equilibrium $R_0(x^*, y^*)$. Moreover, the bifurcation diagrams with respect to τ shown in Figure 8A reveals that the existence interval of pseudo-equilibrium is an increasing function of τ. In this case, the pseudo-equilibrium R_0 is stable with respect to the sliding segment Σ_s. All these results confirm that the larger τ, the more easily does the system stabilize at the pseudo-equilibrium R_0, i.e., the number of pests finally stabilizes at the ET, as shown in Figures 8D and 8E. Note that for the untreated subsystem S_1, the solution may exceed the EIL resulting in a pest outbreak. However, if we choose the appropriate ET such as $ET_i (i = 1, 2, 3, 4)$ shown in Figures 8D and 8E such that there exists the pseudo-equilibrium $R_0 \in \Sigma_s$, we can see that the number of pests is not only less than EIL, but also can be stabilized at the pseudo-equilibrium R_0. Moreover, the lower is ET, the lower is the number of pests.

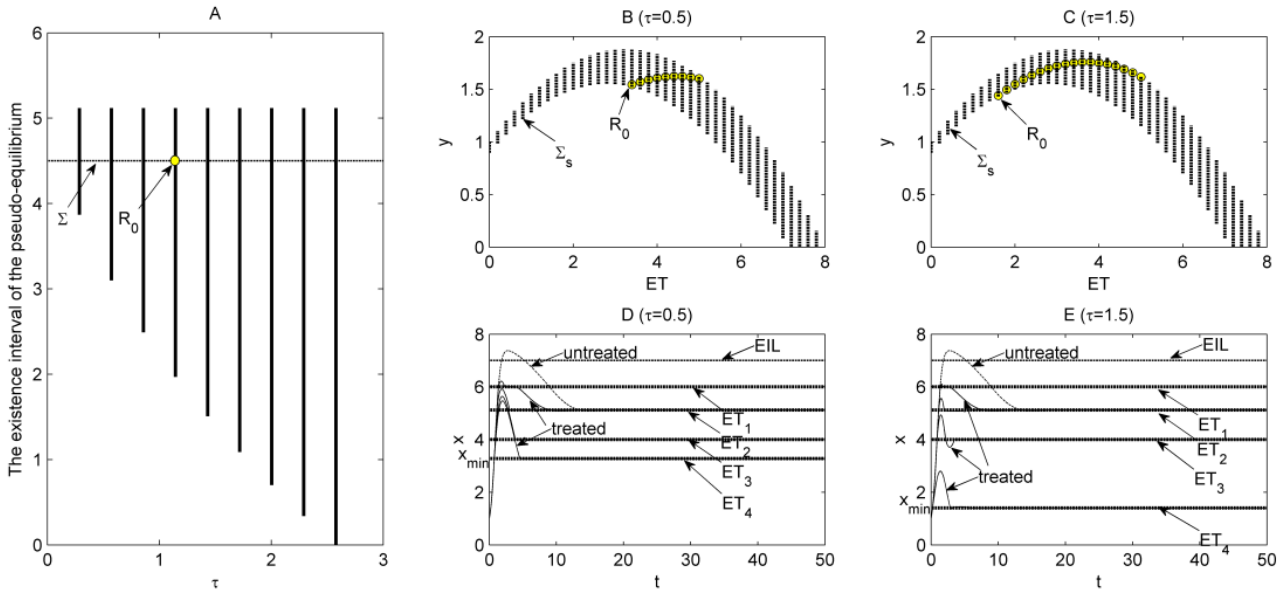

Figure 8. The effects of releasing constant τ on the existence interval of the pseudo-equilibrium R_0 with respect to parameter ET, where the vertical thick segment for each fixed τ represents the interval of $ET \in [x^1_{S_2}, x^2_{S_1}]$ within which the pseudo-equilibrium R_0 exists. The parameter values are fixed as follows: $K = 8$, $r = 3$, $\beta = 3$, $\eta = 5/6$, $\omega = 2/3$, $\delta = \delta_1 = 2.9$ and $\alpha = 1/3$. B: $\tau = 0.5$. C: $\tau = 1.5$. D: $\tau = 0.5$. E: $\tau = 1.5$.

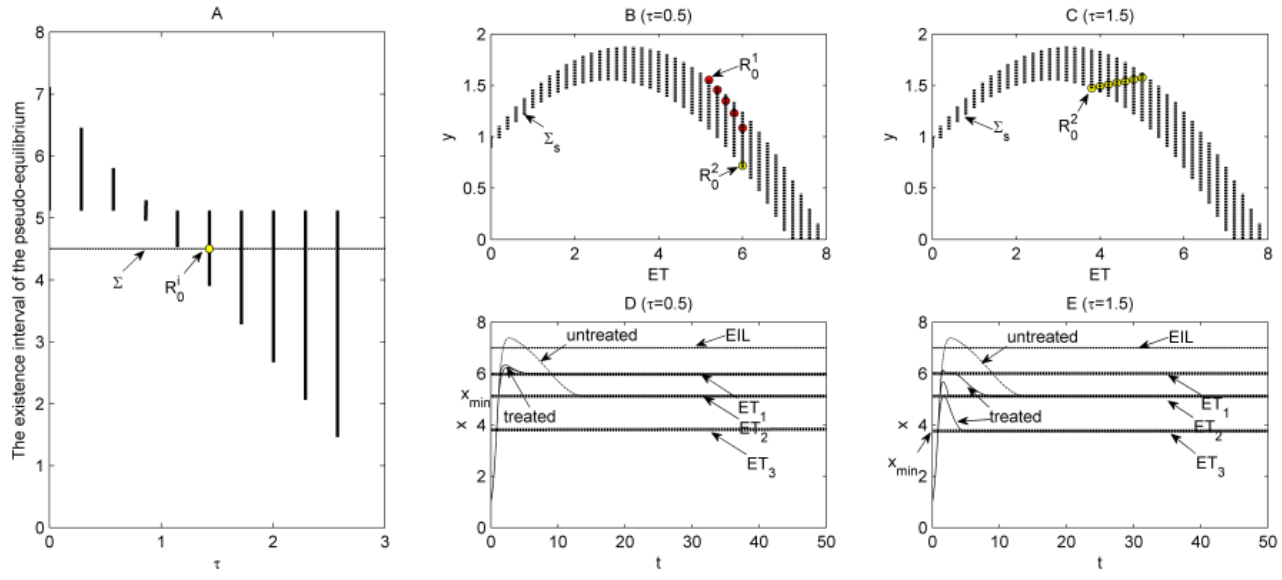

Figure 9. The effects of releasing constant τ on the existence interval of the pseudo-equilibrium R_0 with respect to parameter ET, where the vertical thick segment for each fixed τ represents the interval ET. The parameter values are fixed as follows: $K = 8$, $r = 3$, $\beta = 3$, $\eta = 5/6$, $\omega = 2/3$, $\delta = 2.9$, $\delta_1 = 3.7$, $\alpha = 1/3$. B: $\tau = 0.5$. C: $\tau = 1.5$. D: $\tau = 0.5$. E: $\tau = 1.5$.

If $\delta_1 > \delta$, i.e., spraying pesticides could kill natural enemies, then the effect of releasing constant τ on the existence interval of the pseudo-equilibrium is complex and there may exist two pseudo-equilibria, as shown in the bifurcation diagrams of Figure 9A,B,C. From these we can see that the existence interval of the pseudo-equilibrium is a non-monotonic function of τ, which indicates that if pesticides can kill natural enemies, then the dynamics (particular sliding dynamics) of system (2.2) could be significantly affected, such as the stabilization level as shown in Figures 9D and 9E. It is interesting to note that although the number of pests in untreated subsystem S_1 could increase and exceed the EIL, as shown in Figure 9D, the final size is less than the treated Filippov system (2.2) due to side effects of the pesticide on natural enemies. And it is easy to obtain that the side effects can be effectively avoided by increasing the releasing constant τ, as shown in Figure 9E, which can maintain the number of pests always below the EIL and realizes the control purpose.

For Case (C_2), it is easy to obtain that $R^0_{S_1}$ and $R^0_{S_2}$ always keep in region S_1, and $R^1_{S_1}$ always lies in region S_2. Hence, $R^0_{S_1}$ is a regular equilibrium for subsystem S_1, $R^0_{S_2}$ is a virtual equilibrium for subsystem S_2 and $R^1_{S_1}$ is a virtual equilibrium for subsystem S_1. Moreover, in this case, $R^2_{S_1}$ disappears. If we choose τ as the bifurcation parameter, then system (2.2) may have multiple positive equilibria such as $R^1_{S_2}$ and $R^2_{S_2}$, as parameter τ varies. And the boundary equilibrium (BE) and pseudo-equilibrium could also appear. For example, if $R^1_{S_2}$ collides with the switching line Σ as parameter τ increases, then a BE appears, as shown in Figure 10. In particular, we have:

(i) if $\tau^*_5 < \tau < \tau^*_6$, then two virtual equilibria $R^1_{S_2}$ and $R^2_{S_2}$ coexist, and $R^1_{S_2}$ collides with $R^2_{S_2}$ at $\tau = \tau^*_6$.

(ii) if $\tau > \tau^*_6$, $R^1_{S_2}$ and $R^2_{S_2}$ disappear simultaneously, and system (2.2) does not exist with any positive equilibrium.

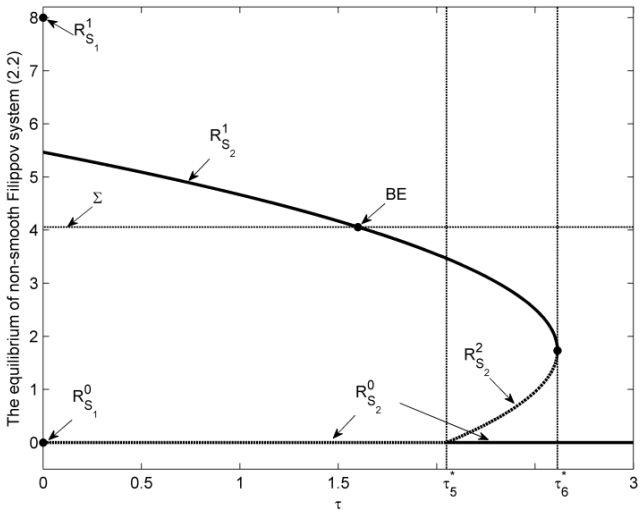

Figure 10. Bifurcation diagram with respect to τ and the effect of parameter τ on the types of the equilibria of Filippov system (2.2). The parameter values are fixed as follows: $K = 8$, $r = 3, \beta = 2, \eta = 1, \omega = 1.5, \delta = \delta_1 = 2, \alpha = 0.95$ and $ET = 4.1$.

Note that the existence and types of equilibria for non-smooth system (2.2) can be discussed by using bifurcation analyses of two subsystems with respect to key parameters (Fig.10), which bring

convenience to the analysis of local bifurcations of the Filippov system, especially those bifurcations related to equilibria. Thus, the local equilibrium bifurcations for other cases can be similarly addressed by employing similar techniques.

4.3.2. Codimension-1 local and global sliding bifurcations analysis

In this subsection, we choose ET as the bifurcation parameter to investigate the codimension-1 local and global bifurcations to analyze the effect of ET on the dynamics of system (2.2). We realize that there may exist similar local and global sliding bifurcations for Cases (C_1), (C_2) and (C_3), so we will take (C_1) as an example to discuss the possible local and global sliding bifurcations in more detail in the following.

For Case (C_1), if $R_1 < 0$, then system (2.2) could have five equilibria $R^0_{S_1}(0,0)$, $R^1_{S_1}(K,0)$, $R^2_{S_1}(x^2_{S_1}, y^2_{S_1})$, $R^0_{S_2}(0, \frac{\tau}{\delta_1})$, $R^1_{S_2}(x^1_{S_2}, y^1_{S_2})$. In particular, if $\delta_1 = \delta$, then $x^1_{S_2} < x^2_{S_1}$, i.e., $R^1_{S_2}$ is on the left of $R^2_{S_1}$, as shown in Figure 7A, which indicates that $R^1_{S_2}$ and $R^2_{S_1}$ can not be the regular equilibria at the same time and it is impossible to have limit cycles on both sides of the Σ. If $\delta_1 \neq \delta$, there may exist rich bifurcations which will be addressed numerically, as shown in Figure 11. It reveals how the ET affects the dynamics of system (2.2), it is easy to see that as parameter ET varies, system (2.2) exists with boundary equilibrium bifurcations and periodic solutions which lie in region S_1 (or S_2). Moreover, there exist other types of periodic solutions including sliding periodic solutions, which include a piece of the sliding segment or the entire sliding segment in Σ; crossing periodic solutions, which only include a point of the sliding segment or without any points of the sliding segment in Σ [17, 23].

In the following part, we begin to discuss boundary equilibrium bifurcations and other types of periodic solutions though the global sliding bifurcations as parameter ET varies, as shown in Figure 11.

Touching bifurcation: A standard piece of the cycle can collide with the discontinuity boundary as parameter ET varies, this bifurcation is called a touching bifurcation (or grazing or even a sliding-grazing bifurcation) [17, 23]. From Figure 11A,B and C, it is easy to see that if $8.45 < ET < K$, there exists a unique and stable cycle (i.e., periodic solution) in region S_1. As parameter ET decreases, the cycle closes to Σ. Especially, when $ET \approx 8.45$, a touching bifurcation occurs, as shown in Figure 11B, where the cycle is tangent to Σ_s at the visible tangent point T_1, denoted by $X_0(x(t), y(t))$. As parameter ET continues to decrease, $X_0(x(t), y(t))$ will contain a piece of the sliding segment in Σ, becoming a sliding cycle (i.e., sliding periodic solution), as shown in Figure 11C with $ET = 8$. The computation of the critical cycle $X_0(x(t), y(t))$, which ends at the visible tangent point T_1, is equivalent to solving the following boundary-value problem, which can be solved by XPPAUT software [37].

$$\begin{cases} \dot{X_0}(x(t), y(t)) = f_1(x(t), y(t)), \\ X_0(T_1) = 0, \\ x(T_{01}) = x(0) = ET, \\ y(T_{01}) = y(0) = \dfrac{r}{\beta} + (\dfrac{r\omega}{\beta} - \dfrac{r}{\beta K})ET - \dfrac{r\omega}{\beta K}ET^2, \\ \langle H_X(T_1), f_1(T_1)\rangle = 0, \end{cases}$$

where T_{01} represents the period of the cycle $X_0(x(t), y(t))$.

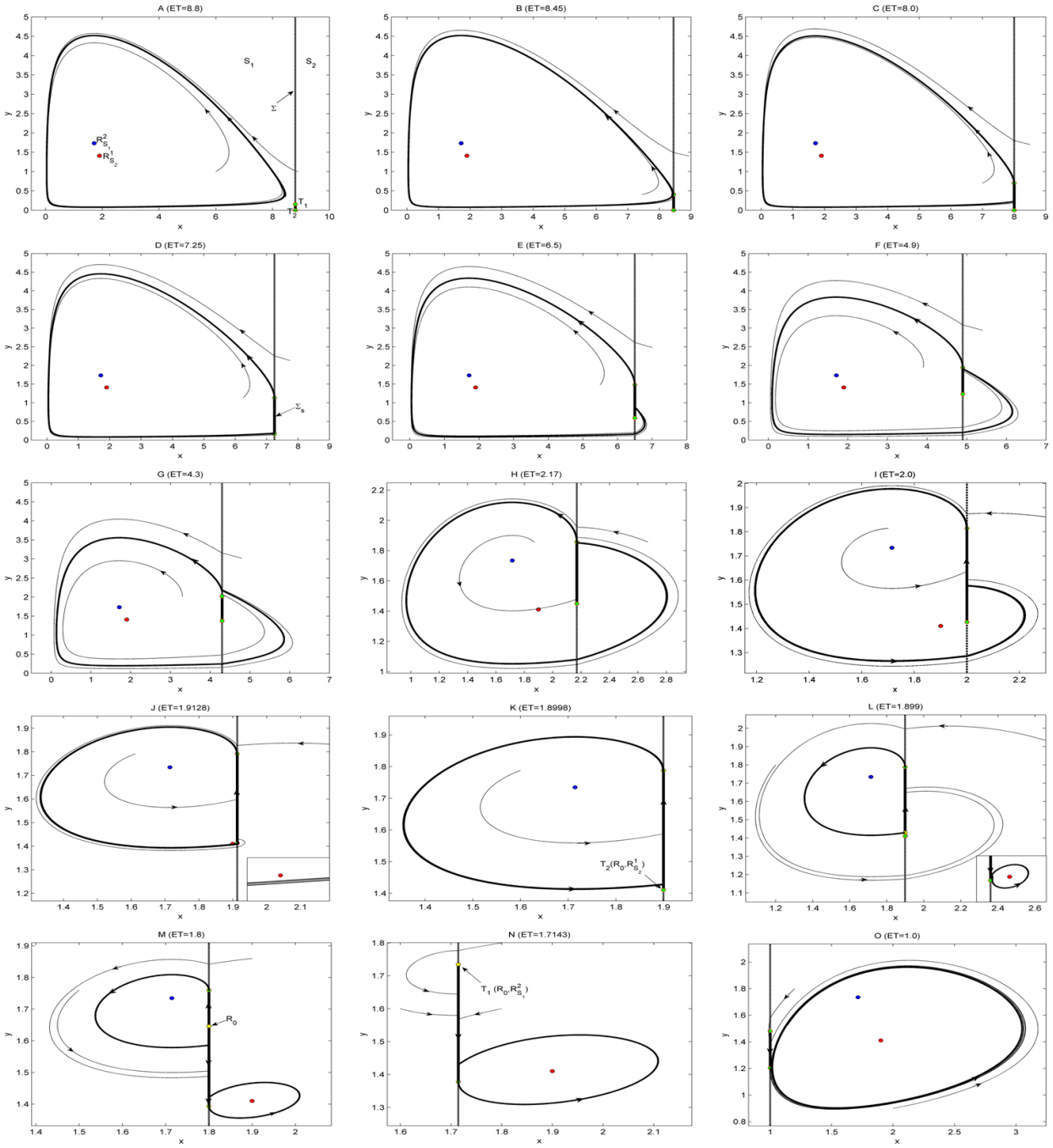

Figure 11. The local and global sliding bifurcations for non-smooth Filippov system (2.2). Here we choose ET as the bifurcation parameter and fix all other parameters as follows: K=9, r=3, $\beta = 3$, $\eta = 5/6$, $\omega = 2/3$, $\delta = 2$, $\delta_1 = 2.45$, $\alpha = 0.5$, $\tau = 0.5$. The local and global sliding bifurcations occur sequentially: touching → buckling → crossing → crossing → buckling → pseudo-homoclinic → boundary equilibrium bifurcations.

Buckling bifurcation: From Figure 11C,D, we can obtain that there exists a stable sliding cycle, which passes the visible tangent point T_1 for $7.25 < ET < 8.45$. As parameter ET decreases, especially $ET \approx 7.25$, the sliding cycle passes the invisible tangent point T_2, denoted by $X_1(x(t), y(t))$. Moreover, it contains the entire sliding segment Σ_s, which means that a buckling bifurcation occurs. As parameter ET continues to decrease, $X_1(x(t), y(t))$ remains but enters into region S_2 before returning back to the sliding segment for $ET > 4.9$, as shown in Figure 11E.

Crossing bifurcation: From Figure 11E,F and G, we can see that a stable sliding cycle becomes a stable crossing cycle as parameter ET decreases. Especially, when ET reaches around 4.9, the sliding cycle only passes one point of the sliding segment Σ_s (i.e., the visible tangent point T_1), denoted by $X_2(x(t), y(t))$. As parameter ET continues to decrease, $X_2(x(t), y(t))$ becomes a stable crossing cycle without any points of the sliding segment Σ_s, as shown in Figure 11G. For the above processes, we say that a crossing bifurcation (or sliding-crossing) has occurred.

Pseudo-homoclinic bifurcation: As parameter ET decreases from 4.3 to 1.9128, the crossing bifurcation and buckling bifurcation occur again, as shown in Figure 11H,I and J. If parameter ET continues to decrease, we can see that when $ET = 1.8998$ (i.e., $ET = x^1_{S_2}$), a stable sliding cycle surrounds the unstable focus $R^2_{S_1}$ and the tangent point T_2 collides with $R^1_{S_2}$ simultaneously. As parameter ET reaches around 1.899, the stable sliding cycle passes the pseudo-equilibrium R_0, which is a pseudo-saddle, forming a homoclinic orbit which contains a piece of sliding segment Σ_s. In this case, we say that a pseudo-homoclinic bifurcation [17, 23] occurs and there are limit cycles on both sides of the Σ, as shown in Figure 11L. In fact, when $ET = x^1_{S_2}$, three points T_2, $R^1_{S_2}$ and pseudo-equilibrium R_0 can collide together. As parameter ET continues to decrease, the three points T_2, $R^1_{S_2}$ and R_0 coexist, and there exists a stable sliding cycle surrounding the unstable equilibrium $R^1_{S_2}$, as shown in Figure 11M. It follows from Figure 11(J-M) that a **boundary equilibrium bifurcation** (or the pseudo-equilibrium bifurcation) occurs at $ET = 1.8998$ (i.e., $ET = x^1_{S_2}$). This bifurcation entails the catastrophic disappearance of a stable sliding cycle and a unstable pseudo-equilibrium R_0.

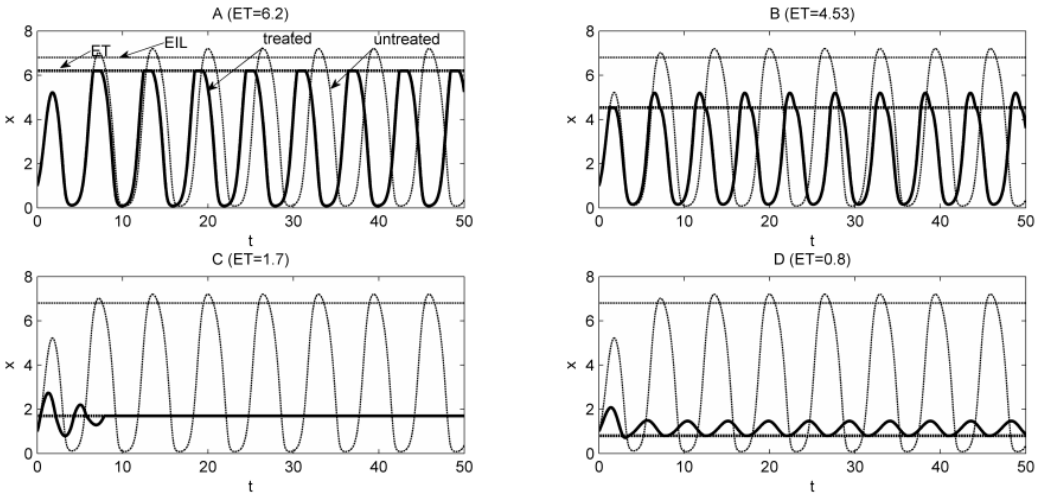

Figure 12. The effects of ET on the number of pests. The parameter values are fixed as follows: K=8, r=3, $\beta = 3$, $\eta = 5/6$, $\omega = 2/3$, $\delta = 2$, $\alpha = 0.5$, $\tau = 0.5$.

Based on the above discussion, we can conclude that when we choose ET as the bifurcation parameter and fix all other parameters of system (2.2), there exist rich local and global sliding bifurcations as follows: touching $\rightarrow$ buckling $\rightarrow$ crossing $\rightarrow$ crossing $\rightarrow$ buckling $\rightarrow$ pseudo-homoclinic $\rightarrow$ boundary equilibrium bifurcations. It is interesting to note that it will cause the change of the regular/virtual equilibria, pseudo-equilibria and trajectories of system (2.2) as ET varies, as shown in Figures 11 and 12. In particular, the results shown in Figure 12 reveal the importance of choosing the threshold level ET. Comparing with the two trajectories of treated and untreated systems shown in Figure12, we conclude that for a given ET, the pest population can be successfully controlled and maintained below the EIL if the IPM is properly designed.

5. Conclusions and discussions

Based on the implementation of biological control in real life, we propose a new non-smooth Filippov system (2.2) with constant releasing rate in this paper. The detailed qualitative analyses for subsystem S_2 were carried out first, which will be crucial for analyzing Filippov system (2.2). Our main results reveal that the releasing constant τ plays an important role in determining the dynamics and bifurcations of subsystem S_2. For example, the threshold conditions for the existence and stability of equilibria and the type of bifurcations including Hopf bifurcation, transcritical bifurcation, saddle-node bifurcation and Bogdanov-Takens bifurcation can be significantly affected by the releasing constant. Moreover, from a pest control point of view there exists a critical releasing rate such that the pest population will be driven to extinction when the releasing rate is greater than the critical value. Meanwhile, compared with the main results obtained in literature [31], we conclude that the sign of the constant τ can significantly affect the dynamical behaviour.

Combining the dynamics of two subsystems S_1 and S_2, and employing the techniques for a non-smooth Filippov system, we focus on some typical cases on system (2.2) with aims to address how the threshold level ET affects the sliding dynamics and pest control [17, 24]. The existence and stability of the sliding mode and pseudo-equilibria have been discussed first, and our results indicate that the releasing constant and side effects of the pesticide on natural enemies could result in multiple pseudo-equilibria. Especially, the existence interval of pseudo-equilibria can be greatly influenced by the threshold level ET and releasing constant τ, as shown in Figures 8 and 9. It is interesting to note that although the number of pests in the untreated subsystem could increase and exceed the EIL, the stabilization level could be less than ET and stabilizes at a lower level than the treated subsystem (i.e., one of stable states of Filippov system (2.2)) due to side effects of the pesticide on natural enemies. In this case, the paradoxical effects of the Volterra principle occur, i.e., spraying pesticide does not reduce the number of pests, but increases them. However, the side effects can be effectively avoided by increasing the releasing constant, which can maintain the number of pests always below the EIL and realizes the control purpose. Furthermore, by numerical bifurcation analyses, the sliding bifurcations including boundary equilibrium bifurcation, touching bifurcation, buckling bifurcation, crossing bifurcation, pseudo-homoclinic bifurcation have been discussed as the threshold level ET varies, which indicates that the pest population can be successfully controlled and maintained below the EIL if the IPM strategy is properly designed, as shown in Figure 12.

In summary, the new model presented in this paper not only has new dynamical behaviour, but also adopts and develops new qualitative techniques. Moreover, the new dynamical behaviour presented in

the model has clear practical significance which can help to guide pest control. Some new non-smooth systems involving the development of pest resistance [38,39] and adaptive control strategy [40,41] will be developed in later research and will be studied in detail.

Acknowledgments

The authors thank Prof Robert A. Cheke for his kind help and comments, thank the anonymous referees and the editor for their helpful comments and valuable suggestions. This work is supported by the National Natural Science Foundation of China (NSFCs, 61772017,11631012,11601301), and by the Fundamental Research Funds For the Central Universities (2018CBLZ001, GK201901008,GK201803006).

Conflict of interest

The authors declare there is no conflict of interest.

References

1. M. E. M. Meza, A. Bhaya and E. Kaszkurewicz, Threshold policies control for predator-prey systems using a control Liapunov function approach, *Theor. Popul. Biol.*, **67** (2005), 273–284.
2. M. I. D. S. Costa and M. E. M. Meza, Application of a threshold policy in the management of multispecies fisheries and predator culling, *Math. Med. Biol.*, **23** (2006), 63–75.
3. S. C. M. Da, Harvesting induced fluctuations: insights from a threshold management policy, *Math. Biosci.*, **205** (2007), 77–82.
4. S. Y. Tang and R. A. Cheke, Models for integrated pest control and their biological implications, *Math. Biosci.*, **215** (2008), 115–125.
5. S. Y. Tang and L. S. Chen, Modelling and analysis of integrated pest management strategy, *Discrete Contin. Dyn-B*, **4** (2012), 759–768.
6. S. Y. Tang and R. A. Cheke, State-dependent impulsive models of integrated pest management (IPM) strategies and their dynamic consequences, *J. Math. Biol.*, **50** (2005), 257–292.
7. G. Y. Tang, W. J. Qin and S. Y. Tang, Complex dynamics and switching transients in periodically forced Filippov prey-predator system, *Chaos, Solitons & Fractals*, **61** (2014), 13–23.
8. A. L. Wang, Y. N. Xiao and R. Smith, Using non-smooth models to determine thresholds for microbial pest management, *J. Math. Biol.*, **78** (2019), 1389–1424.
9. M. I. D. S. Costa and L. D. B. Faria, Integrated pest management: theoretical insights from a threshold policy, *Neotrop. Entomol.*, **39** (2010), 1–4.
10. L. M. Wang, L. S. Chen and J. J. Nieto, The dynamics of an epidemic model for pest control with impulsive effect, *Nonlinear Anal-Real*, **3** (2010), 1374–1386.
11. R. Mu, A. R. Wei and Y. P. Yang, Global dynamics and sliding motion in A(H7N9) epidemic models with limited resources and Filippov control, *J. Math. Anal. Appl.*, **477** (2019), 1296–1317.

12. M. Biák, T. Hanus and D. Janovská, Some applications of Filippov's dynamical systems, *J. Comput. Appl. Math.*, (2013), 132–143.

13. F. Dercole, A. Gragnani, Y. A. Kuznetsov, et al., Numerical sliding bifurcation analysis: an application to a relay control system, *IEEE T. Circuits-I*, **50** (2003), 1058–1063.

14. F. Dercole and Y. A. Kuznetsov, SlideCont: An auto97 driver for bifurcation analysis of Filippov systems, *Acm T. Math. Software*, **31** (2005), 95–119.

15. Y. X. Chen and L. H. Huang, A Filippov system describing the effect of prey refuge use on a ratio-dependent predator-prey model, *J. Math. Anal. Appl.*, **2** (2015), 817–837.

16. J. W. Qin, X. W. Tan, X. T. Shi, et al., Dynamics and bifurcation analysis of a Filippov predator-prey ecosystem in a seasonally fluctuating environment, *Int. J. Bifurcat. Chaos*, **29** (2019).

17. S. Y. Tang, G. Y. Tang and W. J. Qin, Codimension-1 sliding bifurcations of a Filippov pest growth model with threshold policy, *Int. J. Bifurcat. Chaos*, **24** (2014), 1450122.

18. S. Y. Tang, J. H. Liang, Y. N. Xiao, et al., Sliding bifurcations of Filippov two stage pest control models with economic thresholds, *SIAM J. Appl. Math.*, **72** (2012), 1061–1080.

19. J. H. Frank, M. P. Hoffman and A. C. Frodsham, Natural enemies of vegetable insect pests, *Fla. Entomol.*, **76** (1993), 531.

20. D. J. Greathead, Natural enemies of tropical locusts and grasshoppers: their impact and potential as biological control agents, *Biological Control of Locusts & Grasshoppers*, (1992), 105–121.

21. J. C. Van Lenteren and J. Woets, Biological and integrated pest control in greenhouses, *Ann. Rev. Entomol.*, **33** (1988), 239–269.

22. J. C. Van Lenteren, Measures of success in biological control of arthropods by augmentation of natural enemies, *Measures of Success in Biological Control*, **3** (2000), 77–89.

23. Y. A. Kuznetsov, S. Rinalai and A. Gragnani, One-parameter bifurcations in planar Filippov systems, *Int. J. Bifurcat. Chaos*, **13** (2003), 2157–2188.

24. F. Dercole, A. Gragnani and S. Rinaldi, Bifurcation analysis of piecewise smooth ecological models, *Theor. Popul. Biol.*, **72** (2007), 197–213.

25. K. Gupta and S. Gakkhar, The Filippov approach for predator-prey system involving mixed type of functional responses, *Differ. Eq. Dyn. Syst.*, (2016), 1–21.

26. M. Antali and G. Stepan, Sliding and crossing dynamics in extended Filippov systems, *SIAM J. Appl. Dyn. Syst.*, **17** (2018), 823–858.

27. R. Cristiano, T. Carvalho, D. J. Tonon, et al., Hopf and homoclinic bifurcations on the sliding vector field of switching systems in R^3: A case study in power electronics, *Physica D*, **347** (2017), 12–20.

28. L. S. Chen and Z. J. Jing, The existence and uniqueness of the limit cycle of the differential equations in the predator-prey system, *Chinese Sci. Bull.*, **7** (1986), 73–80.

29. M. A. Aziz-Alaoui and M. D. Okiye, Boundedness and global stability for a predator-prey model with modified Leslie-Gower and Holling-type II schemes, *Appl. Math. Lett.*, **16** (2003), 1069–1075.

30. Z. F. Zhang, T. R. Ding, W. Z. Huang, et al., Qualitative Theory of Differential Equations, Science Press, Beijing, 1985.
31. D. M. Xiao and S. G. Ruan, Bogdanov-Takens bifurcations in predator-prey systems with constant rate harvesting, *Fields Institute Communications*, **21** (1999), 493–506.
32. A. F. Filippov, Differential equations with discontinuous righthand sides, Kulwer Academic Publishers, Dordrecht, The Netherlands, 1988.
33. S. Y. Tang and Y. N. Xiao, Biological Dynamics of Single Species, Science Press, Beijing, 2008.
34. Y. A. Kuznetsov, Elements of Applied Bifurcation Theory, 2^{nd} edition, Springer, New York, 1998.
35. L. Perko, Differential Equations and Dynamical Systems 3^{rd} edition, Springer, New York, 1996.
36. H. J. Cai, Y. J. Gong and S. G. Ruan, Bifurcation analysis in a predator-prey model with constant-yield predator harvesting, *Discrete Conti. Dyn- (DCDS-B)*, **18** (2014), 2101–2121.
37. S. R. Lubkin, Simulating, analyzing, and animating dynamical systems: A guide to XPPAUT for researchers and students by Bard Ermentrout, *SIAM Rev.*, **45** (2003), 150–152.
38. J. H. Liang, S. Y. Tang, J. J. Nieto, et al., Analytical methods for detecting pesticide switches with evolution of pesticide resistance, *Math. Biosci.*, **245** (2013), 249–257.
39. J. H. Liang, S. Y. Tang, R. A. Cheke, et al., Adaptive Release of Natural Enemies in a Pest-Natural Enemy System with Pesticide Resistance, *B. Math. Biol.*, **75** (2013), 2167–2195.
40. S. S. Ge, C. Wang and T. H. Lee, Adaptive backstepping control of a class of chaotic systems, *Int. J. Bifurcat. Chaos*, **10** (2000), 1149–1156.
41. C. Y. Gong, Y. M. Li and X. H. Sun, Adaptive backstepping control of the biomathematical model of muscular blood vessel, *J. Biomath.*, **22** (2007), 503–508.

AIMS Press